2. ACCELERATOR AUGMENTATION PROGRAM

2.1 LINAC

S. Ghosh, B. K. Sahu, A. Pandey, A. Rai, P. Patra, J. Karmakar, B. Karmakar, G. K. Chowdhury, D. S. Mathuria, R. N. Dutt, M. Jain, A. Sharma, S. S. K. Sonti, K. K. Mistry, A. Sarkar, R. Joshi, R. Ahuja, R. Kumar, S. K. Suman, J. Chacko, A. Chowdhury, S. Kar, S. Babu, M. Kumar, S. Sahu, J. Antony, J. Zacharias, P. N. Prakash, T. S. Datta, and D. Kanjilal

2.1.1 Operational status of the superconducting linac

The superconducting (SC) linac of IUAC consists of five cryostats containing 27 niobium quarter wave resonators. Since the last few years, energized ion beams from linac are being delivered routinely for scheduled experiments. During the last linac operation in 2014, all the resonators installed in the five cryostats (the superbuncher cryostat followed by three accelerating modules and the rebuncher cryostat) were used in the acceleration and delivery of the ion beam on the target with an energy gain of 8 MeV/q and a time width of ~ 180 ps [1]. Details of accelerated beams are given in Table 2.1.1. The total number of resonators required for the complete linac is twenty seven, twenty six of them were installed in the five cryostats during this test and twenty five of them were used in the beam acceleration. their performance.

Table 2.1.1. The beam species accelerated through Pelletron and SC linac

Beam	Energy from Pelletron (MeV)	SB field parameters	Δt at linac entrance	Energy gain (MeV)			Total energy (MeV)	E_a of RB (MV/m)		Δt at NAND
		E_a (MV/m)		LC#1	LC#2	LC#3		RB1	RB2	
$^{28}Si^{12+}$	130	0.88	117 ps	37.2	31.1	22.2	220.5	-	-	-
$^{48}Ti^{14+}$	162	0.79	160 ps	45.8	39.0	28.2	275.0	2.0	1.0	185 ps

Presently, a few major efforts are dedicated to improve the operational performance of the SC linac. The first one is to improve the accelerating fields of the resonators at 4 and 6 W of helium power. To achieve this, the conventional procedure like more cycles of electro-polishing followed by prolonged rinsing with 18 MΩ-cm de-ionized water is being followed. To improve the quality and efficiency of the rinsing procedure, a new high pressure rinsing facility inside a class 100 clean room has been installed to rinse the resonator just prior to its installation in the cryostat.

The effort is also dedicated to bridge the gap between the accelerating fields achieved during Q measurement at 6 W of helium power and during phase locking of the SC resonator. The major reason behind the inability to phase lock a SC resonator at a field obtained at 6 W of helium power with ≤ 120 W (up to 120 W was proved to be safe for our system in long term operation) of forward RF power is the requirement of large stored energy [0.11 J/(MV/m)^2] and the presence of good amount of microphonic vibration coupled to the resonator. When the microphonic vibration is coupled, mostly, it induces the vibration on the central conductor, niobium tuner bellows and the overall outer body of the resonator. To reduce the vibrational effect and hence the frequency jitter around the locked frequency of the resonator, a couple of steps to reduce the vibration of the central conductor and the niobium bellow tuner have been implemented.

A. Reduction of vibrational mode contributed by the central conductor

To reduce the vibrational mode resonating at ~ 60 Hz, the co-axiality of the central conductor (CC) with respect to the niobium housing of all the resonators were checked and corrected [1]. Then an

improved vibration damping mechanism has been adopted in all the indigenous QWRs built in-house [1]. The details are given below.

(i) Co-axiality of the central conductor with respect to the outer cylinder of the resonator

The central conductor (CC), if it is not co-axial with respect to the outer cylinder produces larger frequency jitter as compared to the fully co-axial CC. To measure the effect of the co-axiality of the CC, the resonator, operated in self excited loop (SEL), was coupled to a fixed amount of external vibration. The Fast Fourier Transformation (FFT) of the frequency difference signal (Δf) between the resonator and a stable reference signal was obtained from the cavity resonance monitor and measured by the spectrum analyser (HP35670A). Fig. 2.1.1(a) shows the large amount of reduction of the amplitude of vibration of a niobium resonator before and after making the central conductor more co-axial (from 5 mm to ±0.5mm).

(ii) Experiments to improve the efficiency of the vibration damper by using SS-balls

In the past, the optimum number and diameter of the SS balls as vibration damper [2] were determined on the resonators fabricated in collaboration with ANL. Later, it was noticed that the surface finish of the inside portion of the end cap of the central conductor (where the SS-ball rests as vibrational damper) fabricated at ANL and the indigenously fabricated ones at IUAC were not identical. So a new series of experiments at room temperature have been conducted to optimize the number and diameter of the SS balls for the indigenously built resonators. The optimum number and diameter necessary to efficiently damp this mode of vibration for the indigenously fabricated resonators are found to be 35 and 8 mm respectively. Figure 1(b) shows the reduction of the vibrational mode around 60 Hz with the modified vibrational damper.

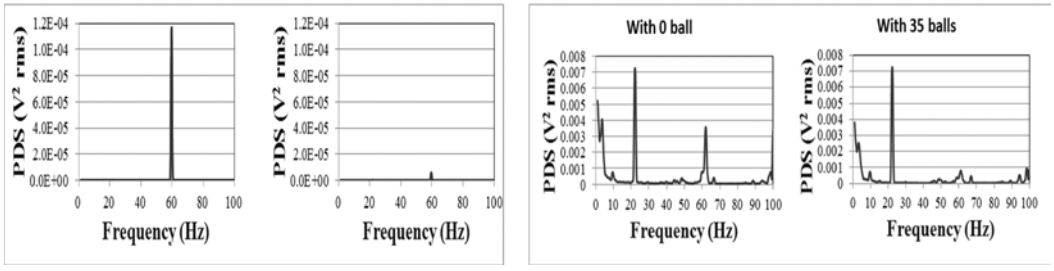

Fig. 2.1.1 Reduction of vibrational mode of frequency (60 Hz)
by making the central conductor more symmetric (a) and by introducing more efficient vibration damper (b).

B. Piezo-actuator as the mechanical tuner and the reduction in the vibrational mode contributed by the bellows tuner

The phase and amplitude lock of the SC QWR at IUAC is achieved with the help of electronic control and mechanical tuner which is correcting the slow drift of the resonance frequency by using pure helium gas to flex the Niobium tuner bellows. In order to improve the dynamics of the existing control, an alternate scheme using piezoelectric actuator based tuner has been developed, tested and finally implemented on all the resonators in the 2nd and 3rd accelerating modules. The control scheme for piezoelectric actuator based control is designed to compensate the slow frequency drift around central frequency of the resonator and also to damp the low frequency eigen-mode excitations during operation. This reduces a substantial load from the dynamic phase control scheme. The comparison of amplitude of vibration of the resonator between gas based and Piezo-tuner is shown in Fig. 2.1.2.

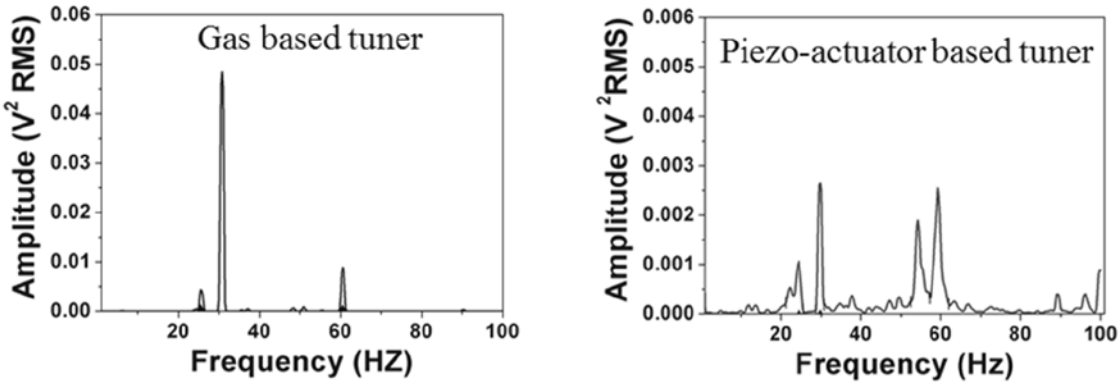

Fig. 2.1.2 Comparison between the gas based and Piezo electric tuner system of resonator.

2.1.2 New developments associated with superconducting linac

A. Completion of class-100 clean room for high pressure rinsing facility and resonator assembly

To achieve the best performance of the Superconducting resonators high pressure rinsing with de-ionized water has become a common practice worldwide. A couple of class 100 clean room, one for high pressure rinsing and another for mounting its accessories on a freshly rinsed resonator, have been fabricated. The facility is going to be used for the final surface cleaning of the resonators prior to their mounting in to the cryostats.

B. Testing of modified pneumatic frequency tuner for linac-I cryostat

Last year a new gas flow control scheme [3] using pulse operated proportional valves was designed and tested in test cryostat in order to improve the dynamics of the existing tuner. The system is now tested successfully on four resonators of linac cryostat-I. This has been found to improve the dynamic response and to ease the phase locking process of the resonators. This scheme will be implemented in all the resonators of linac-1 with a modular electronics control.

C. Installation of capacitive pick up units for beam diagnostic during linac run

Three capacitive pickups have been now installed in the Linac beam line. One has been installed at the entrance of the first accelerating module and the other two have been installed at the linac exit. They will be used for the measurements of the bunch width and the beam energy measurements respectively. The devices will take part during the linac operation in 2015.

REFERENCES

[1] S. Ghosh *et al.,* Proceedings of 27th Linear Accelerator Conference, Geneva, Switzerland, 31 Aug – 5 September 2014, pp. 640.

[2] S. Ghosh, P. Patra, B. K. Sahu, A. Rai, G. K. Chaudhari, A. Pandey, D. Kanjilal and A. Roy, Phys. Rev. ST Accel. Beams 10, 042002 (2007).

[3] A. Pandey et. al., Proceedings of SRF2013, Paris, France, September 2013, PP. 1107-1009.

2.1.3 Superconducting niobium resonators

P. N. Prakash, K. K. Mistri, S. S. K. Sonti, A. Rai, J. Antony, J. Sacharias and D. Kanjilal

The low beta resonator (LBR), designed and prototyped for the superconducting low beta module

(LBM) that will be a part of the proposed high current injector (HCI), was tested at 4.2 K after further processing. The LBR produced very high accelerating gradients, far exceeding the nominal design goal. Initial work on the beam optics design for the HCI-LBM-superconducting linac and Pelletron-LBM-linac combinations has started. Fabrication of the niobium Single Spoke Resonators (SSR1) for Fermi National Accelerator Laboratory (FNAL) has been successfully completed. The resonators have been shipped to FNAL. Development of a 650 MHz, β=0.6 single cell niobium cavity in collaboration with Variable Energy Cyclotron Centre (VECC), Kolkata has been started. The electron beam welding machine has been upgraded and over-hauled, and upgradation of the high vacuum furnace facility has been initiated.

2.1.3.1 Low beta resonator

The niobium low beta resonator, designed and prototyped for the superconducting low beta module that will be a part of the HCI project, was tested at 4.2 K after further processing to remove an additional 40 μm niobium material from the RF surface. In figure 1 the Q-Curve obtained in this run is shown. The resonator achieved the following CW accelerating gradients: 6.2 MV/m with 2 W input RF power, 8.3 MV/m with 4 W, 9.5 MV/m with 6 W, and a maximum gradient of 11.2 MV/m with 13.5 MV/m RF power. The peak surface electric field at the maximum CW gradient of 11.2 MV/m corresponds to 38.5 MV/m. In pulsed mode, the resonator achieved a maximum gradient of 14 MV/m at a duty cycle of 10%.

Although the accelerating gradient achieved in the low beta resonator at 6 W RF input power far exceeds the nominal design goal (5-6 MV/m), we plan to further process the resonator and perform a cold test again. In the proposed test, we plan to perform helium pulse conditioning (HePC), in addition to the high power pulse conditioning (HPPC). We expect that further processing of the resonator will improve its low field performance. Also, HPPC followed by HePC will improve the high field performance beyond 10 MV/m CW gradient (see X-Ray data in Fig. 2.1.3).

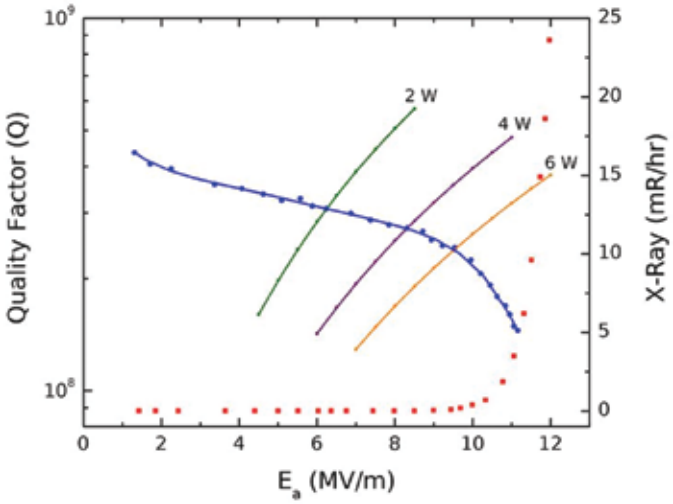

Fig. 2.1.3 Quality factor Q as a function of accelerating gradient Ea in MV/m measured at 4.2 K in the prototype niobium low beta resonator

2.1.3.2 Single Spoke Resonators

The two Niobium Single Spoke Resonators (SSR1; β=0.22, f=325 MHz) being developed at IUAC for Project-X (now called PIP-II) of Fermi National Accelerator Laboratory (FNAL), USA, have

been successfully completed. Before attaching the End Walls to the Outer Shell, the resonators were tuned to the correct frequency by trimming the niobium Outer Shell in steps (thus changing the length of the accelerating gaps) and measuring each time the resonance frequency of the resonators. After the End Walls were attached, four Bridge Ribs were tack welded to each Outer Shell. In Fig. 2.1.4, the completed SSR1 resonators are shown. The two resonators have been shipped to Fermi Lab, where they will be tested.

Fig. 2.1.4 The two niobium Single Spoke Resonators - SSR1 successfully built at IUAC

2.1.3.3 Facility upgradation

The in-house facilities to fabricate superconducting niobium resonator were commissioned at IUAC in early 2002. In the last couple of years they have started to show ageing effects, especially the electronics items. In order to maintain the capability to develop new resonator designs, developments and spares, it was felt that these facilities needed to be upgraded / modernized. This year the electron beam welding (EBW) facility was upgraded and overhauled to make it reliable. A new PC and touch screen, control software supported by a new CNC and PLCs have been incorporated. This required major changes in the electronics and wiring in the gun electronics rack. The electron gun assembly was completely overhauled by replacing the insulator assembly for the high voltage cables with a newer design, gun oil, new heat exchanger for the oil cooling system and high voltage cables. A new colour camera with recording facility was also incorporated in the gun assembly. In addition, both the diffusion pumps were dismantled cleaned and their oil replaced. All mechanical vacuum pumps, isolation valves, pneumatic valves, gauges etc. were serviced. Most of the O-rings in the system were replaced. A new pendant with jogging controls was added to aid the operator in setting up of the job. All the mechanical drives were checked and serviced and where required; components were replaced. The EBW upgradation work took about 5 weeks to complete.

This year, the upgradation of the high vacuum furnace (HVF) has been initiated. It is proposed to integrate the furnace facility and the adjacent surface preparation lab (SPL). For this, the civil works have already started. It is proposed to completely overhaul the various systems in HVF including

the vacuum pumps, valves, gauges, interlocks, cooling circuit etc., and by replacing the existing control system with modern hardware (PC, PLCs etc.) and SCADA software. It is also proposed to attach a dedicated RGA on HVF for online monitoring during the heating cycle.

The upgradation and modernization works in SPL will be taken up this year.

2.1.3.4 Single cell β=0.6, 650 MHz niobium cavity

Under the Indian Institutions and Fermi Lab Collaboration (IIFC), VECC and IUAC are developing a β=0.6, 650 MHz single cell niobium cavity. The cavity components will be formed and machined by VECC and electron beam welded at IUAC. Initial discussions on process development, methodology, fixture design, surface preparation etc. are completed. The first niobium cavity is expected to be ready in the next couple of months.

2.2 HIGH CURRENT INJECTOR

The High Current Injector (HCI) Project will accelerate the ion beam from ECR source using normal temperature Radio-Frequency Quadrupole (RFQ), IH type Drift Tube Linac (DTL) and superconducting low beta cavity module to match the input velocity at our existing superconducting linear accelerator. The HCI is in the advance stage of fabrication.

Few changes are proposed for implementation in LEBT and MEBT sections. The chopper and TWD are being designed to provide different repetition rate of ion beam bunches based on user requirement. The planned repetition rates are 250 ns, 500 ns, 1 μs, 2 μs, 4 μs and 8μs. The LEBT section will be modified to accommodate chopper and TWD systems.

2.2.1 High temperature superconducting ECRIS-PKDELIS and low energy beam Transport (LEBT)

G. Rodrigues, Y. Mathur, P. Barua, A. Kothari, M. Archunan, Chandrapal, R. Ahuja, A. J. Malayadri, U. K. Rao, R. N. Dutt, A. Mandal and D. Kanjilal

A. Installation of the 18 GHz high temperature superconducting ECR ion source, PKDELIS and low energy beam transport system on the 200 kV high voltage platform

The 18 GHz high temperature superconducting ECR ion source, PKDELIS and the low energy beam transport system have been installed on the 200 kV high voltage platform, as shown in the left hand side of Fig. 2.2.1. The beam transport components before the analyzing magnet are the indigenously made, movable, multi-electrode extraction system, magnetic steerer and an electrostatic quadrupole doublet. The electrostatic quadrupole doublet is used for transporting the beam through the magnet at a slightly low field to achieve double focusing. Immediately after the analyzing magnet, a diagnostic box consisting of a beam profile monitor, double slits and a Faraday cup are mounted inside the box in a compact manner. This also serves the purpose to measure the beam intensity due to the large emittance from the ion source. Further downstream, a magnetic steerer and a quadrupole triplet serves to transport and focus the beam at the waist position of the multi-harmonic buncher.

The initial beam tests are being carried out to test the parameters of the ion source and the low energy beam transport system. The control of all the parameters are being accomplished from a control system based on VME fastbus (Fig. 2.2.2).

Fig. 2.2.1 (left) View of the 200 kV high voltage platform; (right) view of the 18 GHz HTS ECR ion source and beam transport components installed on the platform.

Fig. 2.2.2 (left) View of the VME based control system; (right) view of the beam at the first beam profile monitor after the analyzing magnet.

The beam optics through the low energy beam transport section is shown in Fig. 2.2.3 for a beam with an intensity of 100 μA.

B. Electronics and related maintenance activities:

(i) Four +/- 10 kV, 2 mA high voltage DC power supplies have been modified at component level to +/- 3 kV, 5 mA rating. These are required for functioning/powering of the electrostatic quadrupole before the analyzing magnet for PKDELIS ECR ion source. They were first tested individually on dummy load at the test bench and then installed in the main system on the high voltage deck/ platform. They are being used regularly for tuning the ion bean from ECR source to Faraday cup 1 (FC1).

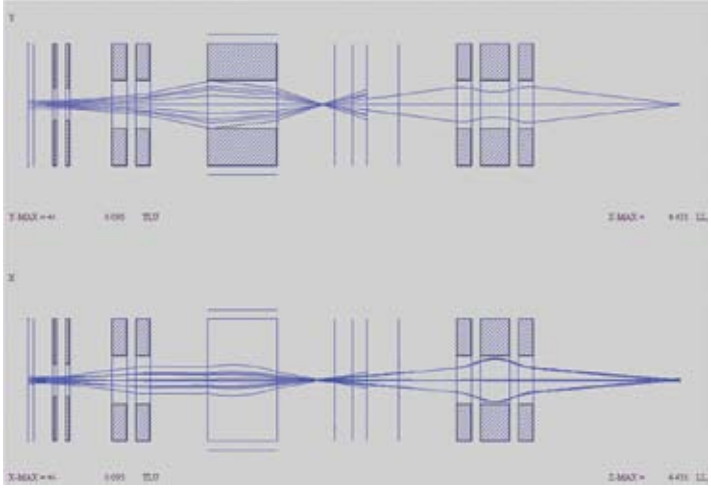

Fig. 2.2.3 Beam optics through the low energy beam transport section

(ii) All the control electronics, electronics related to the ECR source power supplies have been shifted carefully taking all necessary precautions from room no. 127 to high voltage deck/platform in beam hall-III. All the power supplies and other electronics were then installed and interfaced with the control system. Safety interlock system has also been implemented and tested by simulating the fault conditions. This system is now functioning satisfactorily.

(iii) Radio modem and MODBUS based modular control system with wireless communication has been assembled in two 4U panel boxes and installed on the high voltage platform in beam hall-III. It has a LabVIEW based user interface console at the operating end. It has been tested successfully while initial tuning of the ion beam from PKDELIS ECR ion source in December 2014.

(iv) The second high voltage deck for PKDELIS ECR ion source which is operated at source potential was modified to accommodate in the available space of the main deck and as per other constraints. This deck is having a bias power supply which is operated with respect the source potential, an oven power supply which can be operated with respect to the dc bias potential, control modules and isolation transformers. This deck has been installed and tested successfully using MODBUS modules with wireless communication and as well as with optical isolation communication using fibre optics. It is being used regularly for tuning the ion beam from PKDELIS ECR ion source.

(v) Two +3 kV, 5 mA high voltage power supplies used for electrostatic quarupole before analyzing magnet were recently found to be faulty. This was causing difficulty in tuning and extracting the beam from ECR ion source to Faraday cup 1. These power supplies had been repaired by replacing the power MOSFET IRF640 and one Schottky diode. These power supplies are now working properly and are being used regularly in tuning the ion beam.

2.2.2 Design and low power RF tests on the modulated 2.5 m RFQ accelerator

Sugam Kumar, R. Ahuja, A. Kothari and C.P. Safvan

A continuous mode 4-rod Radio Frequency Quadrupole (RFQ) with operating frequency of 48.5 MHz is designed and constructed as an accelerator section of High Current Injector (HCI) system to accelerate ions with A/q of 6 from 8 keV/A to 180 keV/A. The ion beams produced by the ECR (PKDELIS) source will be injected into the RFQ and be further accelerated to just above 2 MeV/A by a drift tube linac (DTL) working at room temperatures, velocity matched beam with $\beta = 0.08$ will be injected into superconducting linac, which will further accelerate the ions to 5 MeV/A. RFQ consists of eight numbers of vane posts and twenty numbers of vanes made of oxygen free copper. Total length of the vanes is 2536 mm and minimum aperture between the vanes is 12 mm. To achieve thermal stability, cooling channels have been provided in vane posts as well as in vanes. The whole

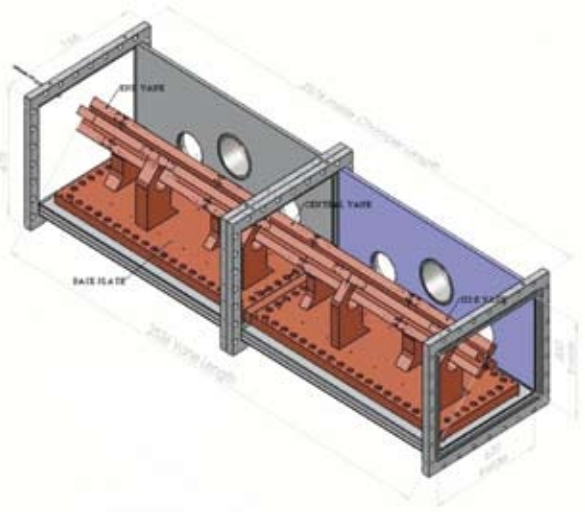

Fig. 2.2.4 A three dimensional inside CAD view of radio frequency quadrupole

vane assembly is installed inside a rectangular cavity (as shown in Fig. 2.2.4) with inner dimension of 620×500×2576 mm. To achieve higher conductivity and hence higher quality factor the inner surface of the cavity is copper plated with a plating of 70 βm thickness.

The beam optics and cavity design was done using LIDOS code and CST Microwave Studio. The 3D CAD drawing of the RFQ electrodes assembly and its cavity for mechanical construction is done using SolidWorks software.

Low power RF tests were done to determine parameters like resonant frequency, quality factor, shunt impedance, power required, electric field mapping and quadrupole symmetry.

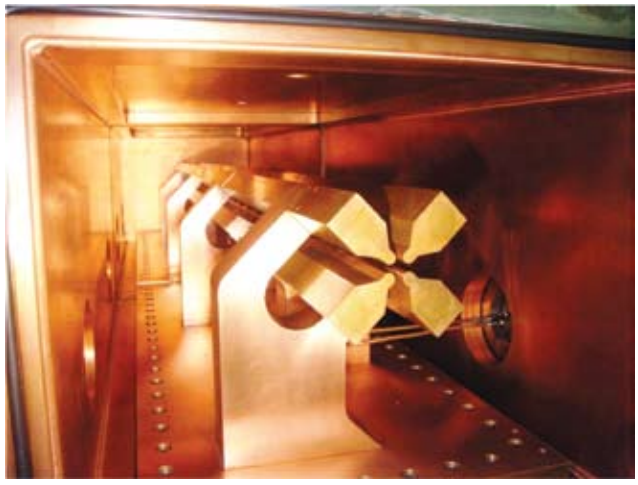

Fig. 2.2.5 Inside view of the installed radio frequency quadrupole

To carry on the RF measurement and to determine the RF parameters we installed a fully automated bead pull system. It's various components like high precision linear and circular rotors, network analyzer and frequency counter were procured, installed and made computer controlled. The other bead pull accessories like dielectric bead, nylon thread and related RF components required for the bead pull measurements were installed. Self-Exciting Loop (SEL) was set up to excite the cavity. SEL was necessary to overcome the temperature drift during long run. We developed various programs using the LabVIEW software to carry on the RF measurements. The resonance frequency was measured to be 44.12 MHz whereas intrinsic quality factor is 5524 which close to design value. The shunt impedance was measured by the capacitive variation method. The shunt impedance comes out to be 87 kΩ.The RF parameters measured are listed below.

Table 2.2.1: RF parameters of final 4-rod RFQ.

Parameters	Ideal	Simulated	Experimental
Resonance frequency	48.5 MHz	-----	44.12 MHz
Quality factor	-----	6000	5524
Shunt impedance	-----	90 kΩ	87 kΩ
Power required	-----	-------	80 kW

To measure the flatness of the electric field along the vane length and the degree of symmetry in the four quadrants, the bead pull method has been used. Two independent measurements have been done in the azimuthal plane along the x-axis and y-axis with 0.1 mm of small step size to check the quadrupole symmetry and the electric field distribution. The electric field distribution is uniform in beam region of ±2 mm. The longitudinal electric field strength is flat within ±6%. The longitudinal electric field profile is shown in Fig. 2.2.6. This small non-uniform distribution in E-field can be reduced by introducing tuner plate between stem. Acceptable limit in field non-uniformity is ±3%.

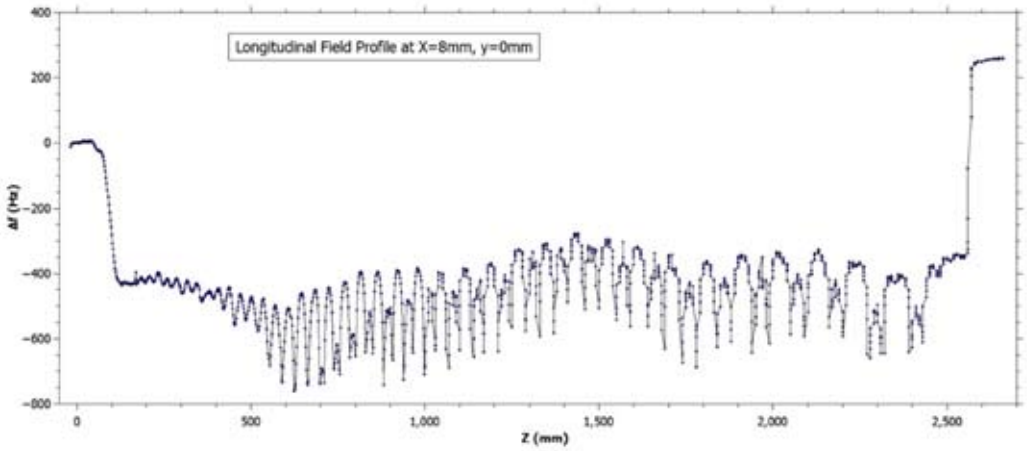

Fig. 2.2.6 Longitudinal electric field profile obtained by placing dielectric bead inside the bore of electrodes and moving it along the beam axis in extremely small steps

Presently we are designing and constructing an automotive inductive tuner for monitoring as well as restoring the resonant frequency of the RFQ cavity during high power tests and beam time operation. Design of RF coupler to feed power up to 100 kW is also under process.

2.2.3 Drift tube linac resonator

Ajith Kumar B. P., J. Sacharias, R. Mehta, V. V. V. Satyanarayana, R. V. Hariwal, S. Kedia, Rajesh Kumar, S. Venkataramanan, B. K. Sahu and P. Barua

The high current injector (HCI) project at IUAC consists of an ECR source, radio frequency quadrupole (RFQ) and a drift tube linac (DTL) to achieve an output energy of 1.8 MeV/u, for ions having $A/q \leq 6$. The RFQ output energy is 180 keV/u and the DTL accelerates it further to 1.8 MeV/u. Acceleration from 180 keV/u to 1.8 MeV/u is done by six independently phased IH type RF cavities. The resonant frequency of first resonator, after fabrication, was found to be at 99 MHz and then it was tested at 5 kW power for 48 days as reported last year. Bead-pull test was also done.

The drift-tube supporting structure was trimmed to bring down the frequency to 97.2 MHz. Two slow tuners, one fixed and another movable, were fabricated and installed. By adjusting the slow tuner the frequency was brought to 97 MHz. The resonator was powered intermittently up to 5 kW for several weeks. After opening some black coating was observed on the end-plates, opposite to the support posts. The tank was cleaned and powered again, under more tight vacuum interlocks. Opening again, the surface was found to be clean.

The power coupler was modified to use ceramic insulator, instead of Teflon. The slow-tuner position is now adjustable using a stepper motor. The supporting structure of the resonator is now based on a Six Strut mechanism, for easy alignment. Mechanical attachments for aligning the end-pates with the drift-tube axis also have been made. Full power tests were done, by maintaining the cavity temperature at around 27o C.

2.2.4 Present status of compact diagnostic system for HCI

R. V. Hariwal, S. Kedia and R. Mehta

A highly compact diagnostic system has been developed for the high current injector. This system is especially designed to measure the beam current and profiles at the entrance of each of the six IH-DTL cavities. The prototype diagnostic system has been fabricated at IUAC workshop and tested with various ion beams in the existing low energy ion beam facility (LEIBF). The diagnostic box consists of Faraday cup and slit scanner to measure the current and profile respectively of the incoming ion beams. Ion beam currents and profiles measured by the compact diagnostic box completely match with the measured values by the National Electrostatic Corporation (N.E.C. USA) made Faraday cup and beam profile monitor (BPM). The online beam test results validated its design and operational aspects in the beamline.

The compact diagnostic box is made of 12 mm thick stainless steel (SS-304) material. As the drift space between two DTL cavities is crucial, to accommodate the diagnostic chamber and quadrupole triplet, we need to minimize the drift. The diagnostic box is of 75 mm longitudinal length which is 1/8th of NEC components size. The radial dimension of the box is approximately 160 mm and the beam aperture is 22 mm. The Faraday cup and slit scanner are mounted in the box in such a way that they are orthogonal to each other. A water cooled Faraday cup has a beam aperture of 22.5 mm and it is 19.5 mm long (Fig. 2.2.7). It is made of Oxygen Free High Conductivity (OFHC) copper material. Based on the expected beam power from HCI the FC is designed for 50 Watts beam power. The suppressor ring, which retains the secondary electrons on the cup, is made of SS 304 material. The FC is completely shielded by the 3 mm thick tantalum sheet. The linear movement of FC is controlled by a pneumatic cylinder, which provides the 60 mm strokes in the diagnostic box. The slit scanner (Fig. 2.2.7) scans the beam in both transverse (x,y) directions with the help of two 500 μm wide slits. The slits are made orthogonal to each other and moves linearly in such a way that they cut the ion beam in x and y directions or vice-versa. The linear motion of the slit scanner is done by a computer controlled stepper motor. The microcontroller programming and data processing have been done with the help of LabVIEW programs. The beam has to pass through one of the slits and to be collected by the cup in the diagnostic box to give the information on beam profile. The diagnostic system is installed in the LEIBF beamline (Fig. 2.2.8) for online beam test.

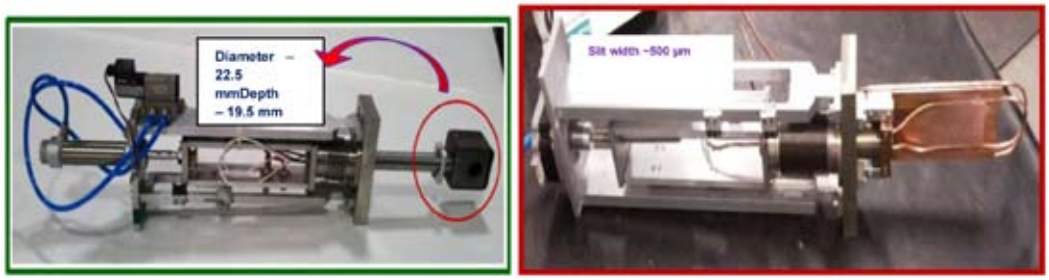

Fig. 2.2.7 Faraday cup and slit scanner

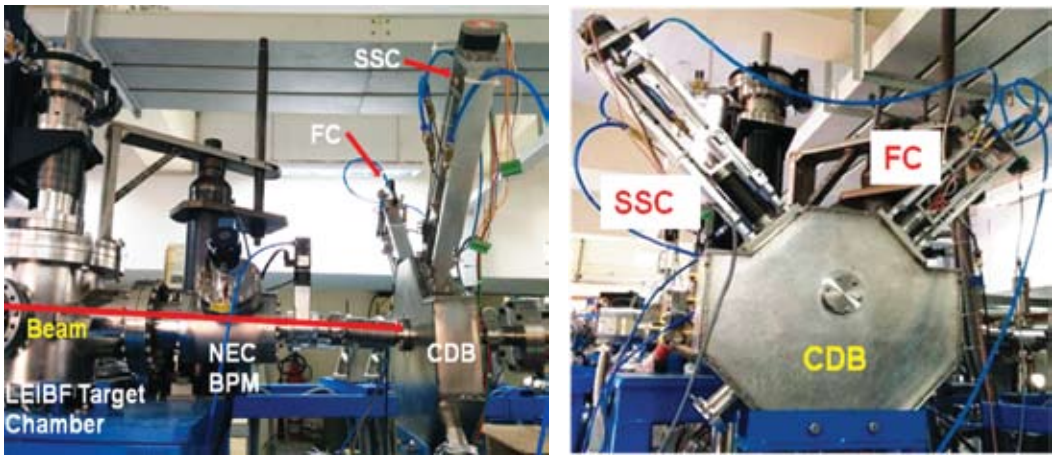

Fig. 2.2.8 Compact diagnostic box installed in LEIBF at IUAC

Argon, oxygen and nitrogen ion beams were tuned to the diagnostic box to measure the current (Table 2.2.2), profile and position (Fig. 2.2.9) at various energy and current. The results matched very well with the standard devices.

Table 2.2.2. Ion beam current measurement by Faraday cup.

Beam	Energy	NEC FC	Faraday Cup
O+5	1.35 MeV	1.6 μA	1.38 μA
N+2	500 keV	1.41 μA	1.28 μA

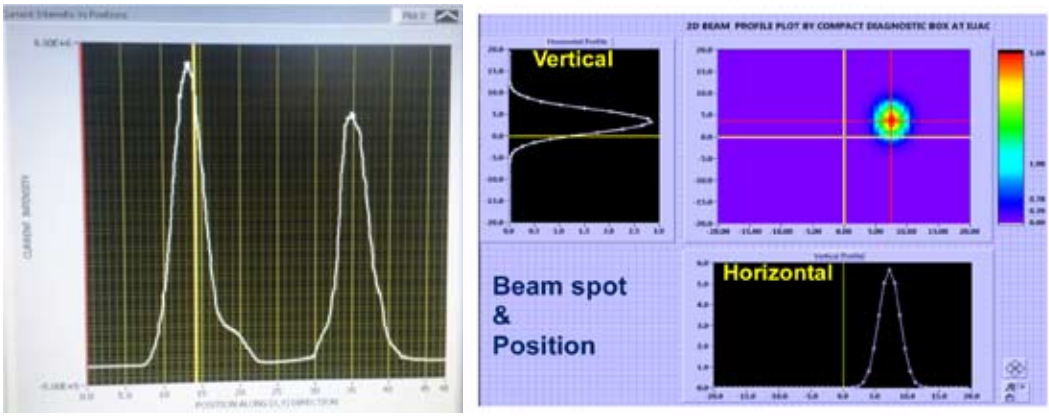

Fig. 2.2.9 Beam profiles

We designed and developed the compact diagnostic system to measure the ion beam current from 1 nA to 100 μA, beam profiles, its positions and spot size. The results validated its accuracy, reliability, easy operation and low cost. On the basis of successful results, we are in the process to make the new diagnostic box compatible with first DTL chamber.

2.2.5 48.5 MHz spiral buncher for MEBT section of HCI

R. Mehta and R. Ahuja

In order to match the longitudinal beam characteristics between the RFQ and the DTL, a rebuncher

cavity is required. As the velocity is low we decided to go with two gap spiral buncher operating at 48.5 MHz though the physical dimensions are comparatively large than 97 MHz, operating frequency of the DTL. The spiral is shorted to the tank at the root and the drift tube is mounted on the other end at the centre of the spiral.

CST MWS and ANSYS were used to determine the desired resonant frequency and the frequency sensitivity of the various mechanical dimensions. One of the major concerns for this type of cavity is the mechanical stability during operation. CST MWS was used to simulate the spiral and obtain the desired resonant frequency with optimum shunt impedance. It was found that a ratio of 2.0 between the widths of the spiral in the xy plane to the pitch of the spiral gave optimum shunt impedance. The ratio of the tank depth to the depth of the spiral in the z-axis (beam axis) also affects the shunt impedance. Although a higher ratio gives higher shunt impedance, the spiral depth was chosen to be 3 cm to provide better mechanical stability.

The buncher has been fabricated and resonance frequency was measured as 48.30 MHz under atmospheric pressure conditions, which matches very well with the designed frequency. The chamber will now be copper platted.

Operating frequency	48.5 MHz
Optimum velocity μ0	0.0196 c
Tank inner diameter	820 mm
Tank length	121.24 mm
No. of spiral section	5
Drift tube ID	10 mm
Drift tube length	40.41 mm

Fig. 2.2.10 Final design parameters for the spiral buncher

2.2.6 Commissioning of power amplifiers for DTL and RFQ

S. Venkataramanan , Rajesh Kumar, V. V. V. Satyanarayana, Y. Mathur , Paramanand Singh, U. K. Rao, A. J. Malayadri, U. G. Naik and R. Mehta

Two power amplifiers, 30 kW at 97 MHz for DTL and 120 kW at 48.5 MHz for RFQ, were procured from M/S QEI Corp., USA. These amplifiers were tested for performance at vendor's site. To commission these power amplifiers at IUAC critical measurements were performed under local conditions such as power utility and cooling system.

Three phase mains power to power the amplifier through suitable switch gear (100 A) and power cable connection was established from temporary electrical panel at HCI beam hall. The cooling water supply to power amplifier and dummy load (30 kw) was provided from nearby manifold.

Dummy load (30 kW) along with 3-1/8" rigid lines, flow rate meter, and water temperature indicator were erected for this purpose.

A. Measured parameters for 30 kW power amplifier

Centre frequency	97.0 MHz
Bandwidth	±1.5 MHz
Power output	30 kW
Phase variations (between 3 kW to 30 kW)	±3°
Harmonic generation	< -36 dBc
Cooling water temperature rise @ 50 lpm	~4°

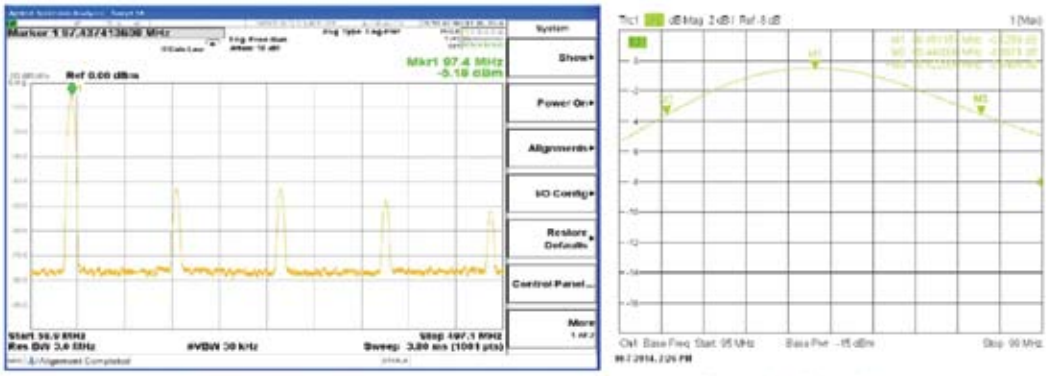

Power Spectral Density at 30 kW

Frequency Gain Transfer Characteristics

Fig. 2.2.11 Test results for 30 kW power amplifier

B. Measured parameters for 120 kW power amplifier

Centre frequency	48.5 MHz
Bandwidth	±350 kHz
Power gain	~86 dB @ 48.5 MHz
Power output	75 kW
Phase variations (between 100 W to 75 kW)	±2°
Harmonic generation	< -36 dBc
Cooling water temperature rise @ 50 lpm	~10°

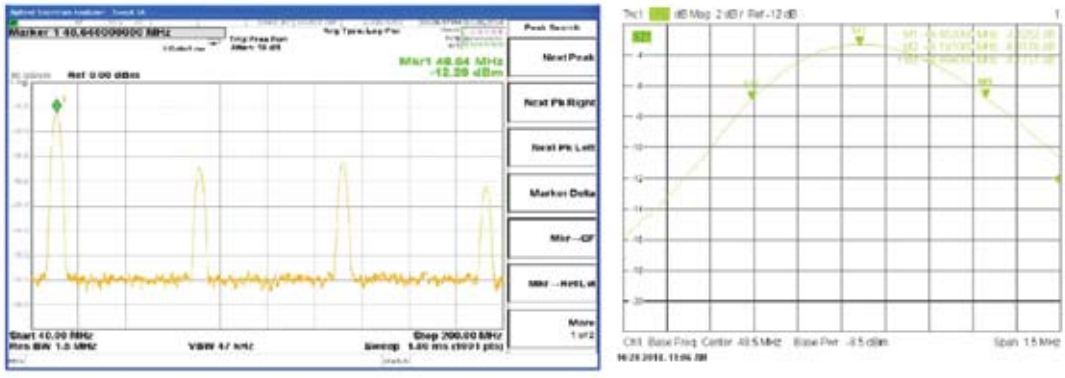

Power Spectral Density at 75 kW

Frequency Gain Transfer Characteristics

Fig. 2.2.12 Test results for 120 kW power amplifier

2.2.7 Beam transport system for HCI

Sarvesh Kumar and A. Mandal

This year, components of the beam transport system of HCI were fabricated as per the beam optics. The dipole magnets were tested for shim angles and homogeneity which agreed well with design values. The quadrupole magnets were tested for magnetic centre and higher order harmonic components. The compact steerer magnets were fabricated and installed in the LEBT section. The transverse beam optics of the whole HCI was done using TRACEWIN from start to end using TRACEWIN code which agreed well with piecewise study using different beam dynamics codes.

2.2.7.1 Testing of first phase of dipole, quadrupole and steerer magnets for HCI

Sarvesh Kumar, A Mandal

The first phase consists of quadrupoles for MEBT section between RFQ and DTL as well as one achromat and two quadrupole triplets in HEBT section. The achromat has two 45o bending magnets with 7 quadrupoles. The magnets have been fabricated by M/s Danfysik, Denmark. The longitudinal field mapping for the magnets in the horizontal plane was performed at both ends of the magnet with 50% and 100% excitation. The effective length was calculated from the field mapping data to get the effective field boundary as shown in Fig. 2.2.13. From the slope of EFB, the shim angles are calculated. Fields are also mapped in the central zone to get the homogeneity. The test results have been summarized in Table 2.2.3. The excitation curve of the dipole magnet is shown in Fig. 2.2.14.

Table 2.2.3. Specifications of dipole magnet and test results

Magnet No.		13178	13179
Parameters	Specifications	Experimental Values	
Homogeneity	~10^{-3}	2.8×10^{-4}	4.0×10^{-4}
Shim angle at the entrance	24° ± 0.5°	24.04°	24.31°
Shim angle at the exit	24° ± 0.5°	24.24°	24.09°

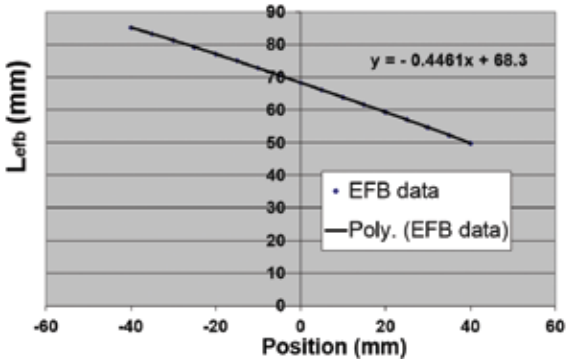

Fig. 2.2.13 EFB for dipole magnet

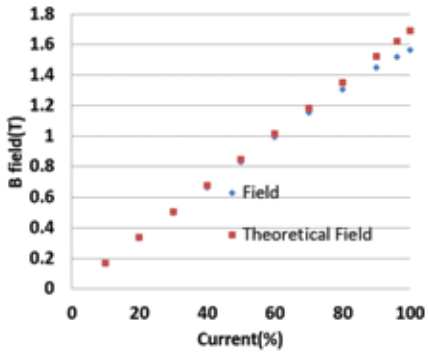

Fig 2.2.14 Excitation curve of dipole magnet

The shim angle on entrance side of the dipole magnet is given as

$$\varepsilon = \tan^{-1} 0.4461 = 24.04°$$

The whole HEBT section has 4 types of quadrupole magnets. There is a common vacuum chamber for quadrupoles and dipole magnets to accommodate their combination in compact space. The design parameters of quadrupoles are given in Table 2.2.4 along with other measured parameters like the harmonic content and the magnetic centre.

Table 2.2.4. Specifications of magnetic quadrupoles and test results

Name	Sr. No.	L_{eff} (mm)	Pole gap (mm)	Gradient (T/m)	Current (A)	Harmonic content (%)	Magnetic centre (mm)	
							ΔX	ΔY
Q1	13171	106	53	18	91.09	1.048	0.04	-0.03
Q2	13166	159	53	18	89.10	0.626	0.18	0.03
Q3	13175	212	53	18	88.50	0.667	0.06	0.02
Q4	13185	318	53	18	88.15	0.390	0.03	-0.01

2.2.7.2 Design of steerer magnets

Sarvesh Kumar, A. Kothari, P. Barua and A. Mandal

A compact steerer magnet is required for small correction of central beam trajectory in LEBT section before the analysing magnet. The design parameters are given in Table 2.2.5 and technical drawing is given in Fig. 2.2.15. The magnet has been fabricated and installed in the beam line.

Table 2.2.5 Design parameters of steerer magnet

SWG No. of Wire of coils	17
Diameter of coils	1.1 mm
Number of turns per layer	71
Number of layers	6
Pole gap	75mm
Maximum magnetic field	100 Gauss
Deflection at 300 mm	±5mm
Physical length of magnet	100 mm

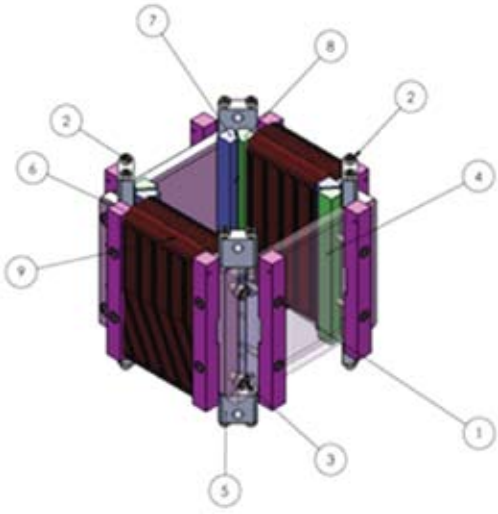

ITEM NO.	PART NUMBER	DESCRIPTION	QTY.
1	M - 4 x 0.7 x 25 Allen Bolt	SS 304	16
2	M - 4 x 0.7 x 30 Allen Bolt	SS 304	16
3	M - 5 x 0.8 x 12 Allen Bolt	SS 304	8
4	SmallYoke	Steel ST37, Chrome Plated	4
5	Smallsupport	Stainless Steel	8
6	SmallNylon Bar	Nylon	8
7	Smallinner Nylon Bar	Nylon	4
8	Smallinner Nylon intersec Bar	Nylon	4
9	Copper Coil, 8 Layers, 54 Turns Each Layer	Cu Coil, Wire Dia = 1.212mm, 18.5 SWG, Medium Covering.	2

Fig. 2.2.15. Technical drawing of steerer magnet

2.2.7.3 Transverse beam optics of HCI

Sarvesh Kumar and A. Mandal

The beam optics calculations have been done piecewise using different codes earlier and presently performed using TRACEWIN code from start to end in envelope mode within framework of linear beam optics regime. A normalised longitudinal emittance of 3 keV/u-ns and normalised transverse emittance of 0.3 π mm-mrad has been assumed at the ECR ion source to design the whole system. The transverse optics is shown in Fig. 2.2.16.

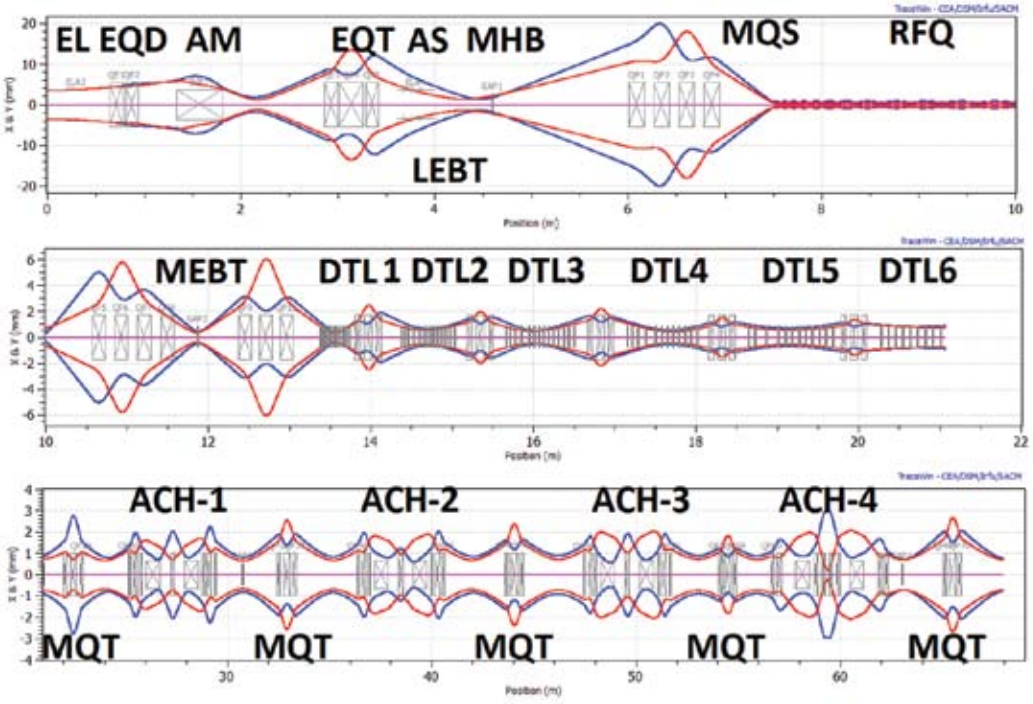

Fig. 2.2.16 Start to end transverse beam optics of HCI by TRACEWIN code

2.2.7.4 Power Supply for HCI Steerer and Low Power Quadrupole Magnets

S. K. Suman, Mukesh Kumar, Rajesh Kumar and A. Mandal

A compact air cooled bipolar current (±10 A) regulated power supply of 400 W has been developed. Series pass transistor controlled linear mode circuit configuration is adopted to regulate the current. The Transistor bank and regulation circuits are designed in such a way that same power supply unit can be operated in unipolar (for quadrupole) as well as bipolar mode (for steerers) by selecting a jumper. For remote control two options CAMAC as well as VME-RS232 is provided.

One prototype power supply has been assembled to check the performance of this design. Several tests were performed to verify the performance such as line and load regulation and long and short term stability. The measured stability is within 100 ppm. After successful testing of first prototype, 30 such power supplies are being fabricated in two phases. In the first phase, 15 power supplies have been fabricated and tested. A few power supplies from the first phase have been installed at the HCI source Deck and LEIBF. The general performance of these power supplies has been very satisfactory. The second phase of the fabrication of the power supplies is going on and will be completed soon.

2.2.8 Development of low level RF (LLRF) control system for DTL and RFQ cavities

Rajesh Kumar, S. K. Suman and V. V. V. Sathyanarayana

The development of LLRF control system for DTL and RFQ cavities has been started in-house. Each cavity will have its own individual control system. The architecture of the control system will be identical for each of the 6 DTL cavities and the RFQ and spiral bunchers. The main functions considered for the control system are controlling the amplitude and phase in open or close loop, controlling frequency tuning in open or close loop and also control and display of the personnel and cavity protection interlocks. For implementing the design the RF signal processing and feedback loops are done using analog circuits, while the set-points, read-backs and interlocking are done using digital circuits. The designed controller is a Generator Driven Resonator (GDR) control, based on amplitude and Phase (A&P) control scheme. PI type analog feed back control loops are used to control the amplitude and phase of the cavity field. Proportional control has been designed to drive a mechanical tuner to control the cavity's resonant frequency to the nominal frequency. The system is designed in a modular way, which eases maintenance and servicing. The electronic circuit boards have all been designed and sent for manufacturing. All the required electronic components have been ordered. The system is currently in the prototype fabrication stage and an operational prototype is expected within a few months.

2.2.9 Development and testing of multi-harmonic buncher (MHB) controller

Rajesh Kumar, S. K. Suman, V. V. V. Sathyanarayana , S. Venkataramanan, Rajan Joshi, Abhijit Sarkar and A. Mandal

A single gap MHB cavity is being developed for injecting bunched beam into RFQ at the upcoming HCI facility. The MHB will be fed with 12.125 MHz sawtooth voltage to have best energy modulation for bunching the DC beam. A prototype Low level RF controller has been developed

which generates 12.125 MHz sawtooth wave with approx. 70% linearity and maintain its phase and amplitude over time. The fundamental (12.125 MHz) and three consecutive harmonics (24.25 MHz, 36.375 MHz, and 48.5 MHz) are mixed in fixed proportion and proper phase to get a sawtooth voltage. The fundamental and the harmonics are individually amplitude and phase regulated before mixing, this enables to mix them in a proper phase and amplitude to get a close approximated saw-tooth. The amplitude and phase are regulated using PI type analog feedback control loops. During last year, extensive measurements were performed to characterize the transfer functions of all the control loops and ways are finalized to close the loops keeping the operating point in the middle of the operating dynamic range. A sawtooth wave of 70 % linearity is generated and regulated against phase and amplitude variations. To power the MHB cavity, a 100 W broad band solid state RF amplifier is driven by using the programmable sawtooth wave generated by the controller. An overall outer feedback control loop has been established by taking feedback from the cavity voltage pickup to regulate the sawtooth shape, amplitude and phase of the cavity field. A separate feedback loop to phase lock the MHB field with beam phase has been implemented. It modulates a system phase shifter depending upon the phase difference between beam pickup signal and master oscillator. The testing of the controller is done in actual setup using Pelletron MHB cavity to validate the design and to accumulate relevant technical data for further optimization of the system before going to the final fabrication (although prototype testing has not been completely finalized at this time of testing). During its first operation, the controller was able to lock the phase and the amplitude of the MHB cavity. Nevertheless, the designated performance, especially the required bunch length as per the liner portion of the sawtooth was not reached. The cavity and beam phase locking was tested by adjusting the steerer before the MHB cavity. The measured variation in the bunch centroid with different beam path is always well within the required stability range. The beam bunches do not show any insignificant tailing.

2.2.10 Development of the MHB for high current injector

R. Ahuja, Sarvesh Kumar and A. Sarkar

2.2.10.1 The mechanical assembly

The total mechanical assembly is now ready for installation in the HCI beam line. The installation will be done any time this year. The 14 inch side cubical vacuum chamber with 6 ports with 2 NEC type flanges and 4 conflat type flanges with the the grid assembly which includes the copper cones and cone extensions were fabricated earlier. The entire grid assembly was aligned successfully and the aligning rods were welded on RF ceramic fluted insulators. The fluted insulators are welded on the top flange and act as RF feed-throughs to carry RF power to the grids. The molybdenum grids were brazed successfully on the copper cones by a very special technique in a vacuum furnace by a Pune-based company.

2.2.10.2 The tank circuits

The tank circuit is complete and ready. It has been mounted on the top plate of the vacuum chamber. The co-axial cooling has been tested successfully. Initial tuning and low power tests are in progress. High power tests will be taken up shortly.

2.2.10.3 The electronics

The new controller which was designed and fabricated earlier, has been tested thoroughly. All the phase lock loops and amplitude lock loops were tested separately before assembling all the modules

in the controller box. Proper power supplies were also assembled in the box. All connections were made and the whole unit was tested by feeding the composite RF output to RF power amplifier. The feedback was taken from the amplifier output through an attenuator. In this way, the sawtooth was successfully generated and controlled by the controller. Presently the controller unit is being tested with the Pelletron-MHB.

2.3 CRYOGENICS AND APPLIED SUPERCONDUCTIVITY LAB

Anup Choudhury, Jacob Chacko, Joby Antony, Manoj Kumar, Santosh Sahu, Soumen Kar and T S Datta

2.3.1 LHe and LN2 plant operation

The LHe machine was operated 4 times (run no 8 – run no 11) during the whole course of the year with only one run in closed loop mode (run no 8). A total of 2200 hrs was clogged on the main compressor. A brief tabulated report on the total runs is shown below.

Table 2.3.1. Operational summary of the LHe plant.

Run no	Date of operation	Hrs on compressor	Usage
8	22/04/14 – 15/06/14	3650 – 4874 (1224 hrs)	Linac operation, Oxford cryostat
9	22/09/14 – 28/09/14	4874 – 5078 (204 hrs)	STC, QC magnet, Oxford cryostat
10	11/11/14 – 01/12/14	5078 – 5600 (528 hrs)	STC, QMC, Oxford cryostat
11	27/01/15 – 06/02/15	5600 - 5844 (244 hrs)	STC, QMC, Oxford cryostat

The linac operation this year was used for calibrating the machine and to know the operational characteristic with different beams. During the course of the run a cold leak developed (slow tuner line) in linac 3 cryostat. The cryostat had to be warmed up while keeping the other cryostat in cold condition. This operation required making a special transfer line with a gas heater connection to warm up the cold gas coming from cool down of the cryostat. The transfer line was fabricated in a very short time. The whole warm up and cool down operation took 2 weeks. All the other plant operations were done for operation for STC (simple test cryostat), quadrupole magnet or oxford made PPMS cryostat. In all the STC operation a custom-made LHe transfer line (2.5 m long) was used to fill the cryostat directly from the 2000 l dewar. Although this operation made the cooling of cryostat easier but we could notice that the cool down time has enhanced resulting in more LHe requirement. Some more studies are planned to identify the source of the heat leak.

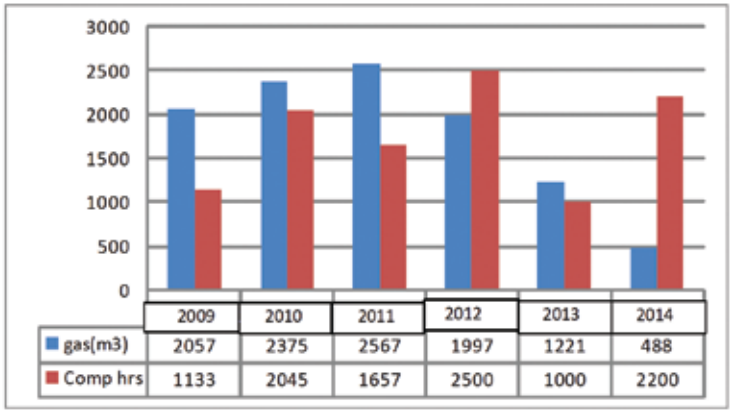

Fig. 2.3.1 Annual helium gas recharge vs compressor running time for the period 2008-2014

One notable issue is the gradual decrease of the annual helium gas consumption after new plant has started operation in 2012 (Fig. 2.3.1) It can be seen from the bar chart that the gas requirement has drastically fallen in the after 2012 indicating that the new LINDE machine has reduced helium leak compared to the old liquefier and also the operation losses has also come down drastically. This year one of the major sub system air drier of the LN2 Plant has been replaced with a new system. The older one was dual type for the same capacity and was giving more troubles due to electronic control related issues. The new one is of KAESER make with higher capacity of 10 m3/h and comparatively has lesser maintenance. The plant with new drier has run satisfactorily throughout the year without any problem.

Fig. 2.3.1 New drier system incorporated in the existing Stirling plant

The total quantity of liquid nitrogen produced during this year was 1,85,000 l whereas 1,45,000 l was purchased from outside to meet the regular requirements and to run linac.

2.3.2 LINAC activities

2.3.2.1 Calibration of dynamic cryogenic load with the RF power in LINAC cryomodule-II (LC-II)

The RF power given in the superconducting cavities in each linac cryomodule gives a dynamic cryogenic load to the helium refrigerator. The RF power in the cavities needs to be varied according to the energy requirement of the accelerated ion beam. In this academic year, the dynamic RF load has been calibrated with the cryogenic load to the 4.2 K refrigerator. Six resistors of 10 Ω@10 W capacity, immersed in the liquid helium bath in LC-II, have been used for the equivalent cryogenic load calibration. Initially, the six cavities in LC-II have been powered in critically coupled condition with total 34 W of power with an average of 5.75 W per cavity. At this dynamic RF load, first the 4.2 K refrigerator has been thermodynamically balanced with a set of process parameter like pressure, temperature and mass flow rate etc. Once the 4.2 K refrigerator reaches

to the equilibrium condition, the dynamic RF power of one cavity in LC-II has been put off which eventually makes the refrigerator thermodynamically imbalanced. The 4.2 K refrigerator has been made to stabilize with same process parameters by powering one of the heaters immersed in the liquid helium bath. Hence the heat power gives the cryogenic load equivalent of the dynamic RF power in the cavities. Similarly, all other cavities are put off one by one and the corresponding RF power has been replaced by the heater to simulate equivalent cryogenic load. The cryogenic load closely agrees with the equivalent RF-power in critical coupled condition.

Similarly, the six cavities in LC-II are powered in over-coupled condition with dynamic load of 85 W per cavity which corresponds 5.5-6 W of equivalent RF power in critical coupled condition. The equivalent total RF power of critical coupled condition is 34 W for six cavities. The cryogenic load closely agrees, with the effective RF-power given in over-coupled condition, less than 10% of deviation.

2.3.2.2 Calibration of liquid helium supply valve with the dynamic RF power in linac Cryomodule-II

The supply valves of liquid helium in all the cryomodules are controlled in PID loop with the liquid helium level. The static heat inleak of each cryomodule will correspond some percentage of opening of supply valve. When RF power is applied to the cavities of the linac cryomodules, the opening of the supply valve increases to compensate the excess cryogenic load or to maintain its liquid helium level using PID loop. The dynamic RF power has been simulated by the heaters immersed in liquid helium bath in LC-II. Fig. 2.3.3 shows the dynamic heat load (RF) versus the liquid helium supply valve opening of the cryomodule. This calibration would greatly help in real time estimation of excess cryogenic load during RF powering of the cavities for ion acceleration.

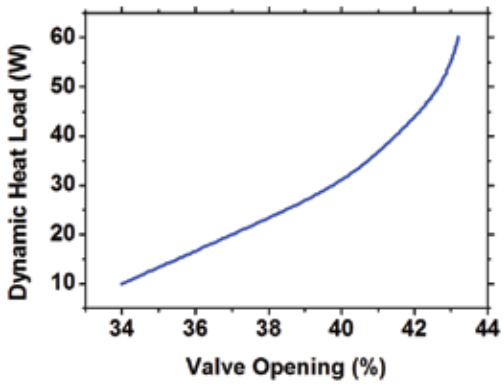

Fig. 2.3.2 Dynamic heat load vs valve opening of linac

2.3.2.3 Distribution line activities

In earlier years of operation, frequent blockade problem of the nitrogen feed control valves of linac II and linac III were observed. The problem of this blockade was identified to be that of having smaller C_v of these valves at the upper end of the flow. Both these valves were replaced with new control valves from WEKA having a C_v of 1 instead of earlier C_v of 0.4. With these new valves both transfer lines were again refabricated. After replacement of the valves, the filling operations have eased and due to higher C_v the cool down of the cryostat shield also has become faster.

2.3.3 Superconducting quadrupole magnet for HYRA

An ever-cooled superconducting quadrupole doublet magnet (using 2 GM cryocoolers) system with a field gradient of 20 T/m and room temperature bore of 200 mm of diameter was commissioned last year. In the last test when both the coils were energized for long duration we found that both the coils quenched after 6-7 hrs simultaneously. One of the HTS of the SQC-250 was found to be opened. This year our efforts were focused in understanding the problems associated with this double quench and rectify them. The HTS to LTS joining of the entire second stage was redesigned

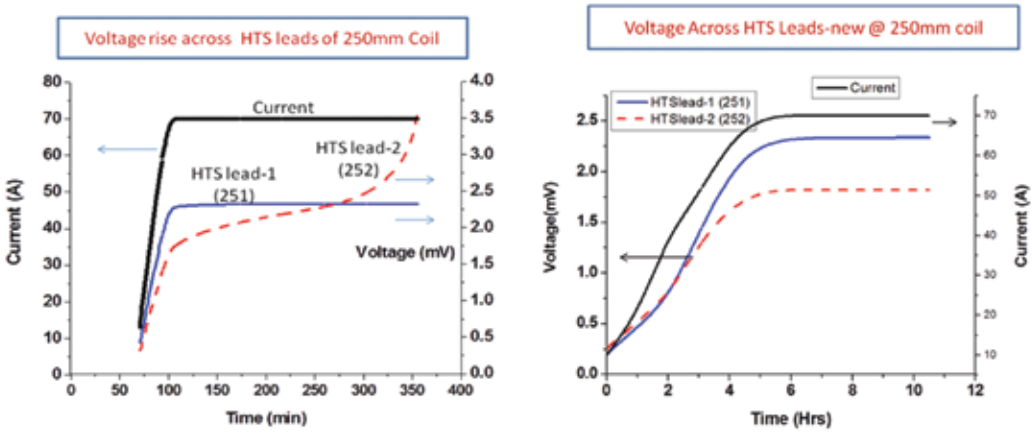

Fig. 2.3.3 I-V curve of the HTS leads (HTS-251 and HTS-252) of the SQC-250 coil during energization up to 70 A

and also the copper to HTS joining (first stage) of the burnt lead was changed. The changing of the HTS to copper joint at the first stage solved the problem of heating of first stage and this solved the problem of quenching in coil SCQ-250. Fig. 2.3.4 shows the voltage profile across the burnt HTS lead before and after the Cu-HTS joint was reconfigured. The voltage rise in the initial curve signifies the thermal growth in the adjoining joint.

During re-energization of SQC-300 coil, a parasitic 20 mΩ resistance has been found across the coil, which was not present earlier. Detail thermal analysis is going on to find out the sequence of events behind the resistance growth.

2.3.4 Other development activities

2.3.4.1 Oxford cryostat reactivation

After a gap of 16 years Oxford make cryostat (ppms measurement system) has been revived again. This involved measuring the static evaporation rate of the cryostat under various conditions,

Fig. 2.3.4 Oxford cryostat setup

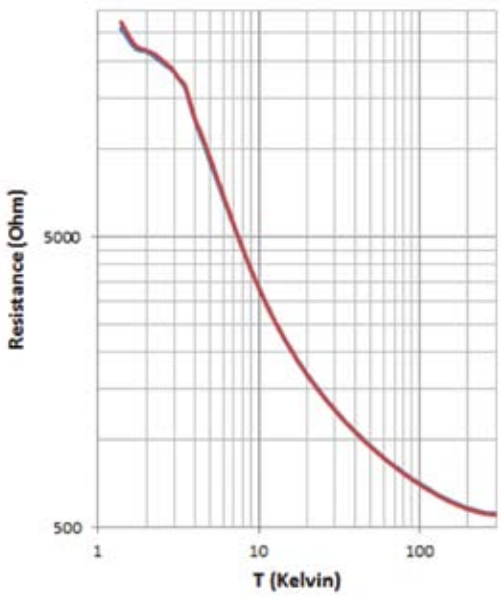

Fig. 2.3.5 Calibration curve

inserting a superconducting LHe sensor inside the dewar with a modified feed through, changing the sealing of the current leads, firmly anchoring them to the body and lastly making a full variable temperature insert (VTI) probe with 22 pin feed through. During the initial cool down the cryostat was tested for its static evaporation rate which was measured to be 400 l/h. When the magnet is energized the evaporation increases by 360 l/h.

The system has been running in closed loop mode for ~20 days (with initial hiccups with VTI and current lead seals). During this period apart from low temperature lab activities we have extensively used the setup to calibrate different kind of diode sensors and Allen Bradly carbon resistors. The full calibration curve for the Allen Bradley resistor is shown in Fig. 2.3.6. It is also worth mentioning that these resistors are very less sensitive to magnetic field and the adjoining graph shows how the calibration graph varies with and without magnetic field at low temperature. With the successful commissioning of the setup we are able to calibrate any temperature sensors from 300 K to 1.5 K in complete automated way.

2.3.4.2 BRNS LN_2 liquefier

A GM cryocooler based nitrogen liquefier has been commissioned last year. Its production capacity is 64 l/d using a Cryomech AL 300 cryocooler. This year the focus was to make the nitrogen generator part using a membrane. This involved separation of nitrogen gas from air using tested membrane module. The parker membrane (model no HiFluxx DT604) was tested for its performance with various pressures and the oxygen impurity level was measured. It is observed that at higher the impurity level comes down for any given flow across the membrane. The whole of this NSM has been assembled to the liquefier and a run was successfully undertaken to verify the projected outcome submitted to BRNS.

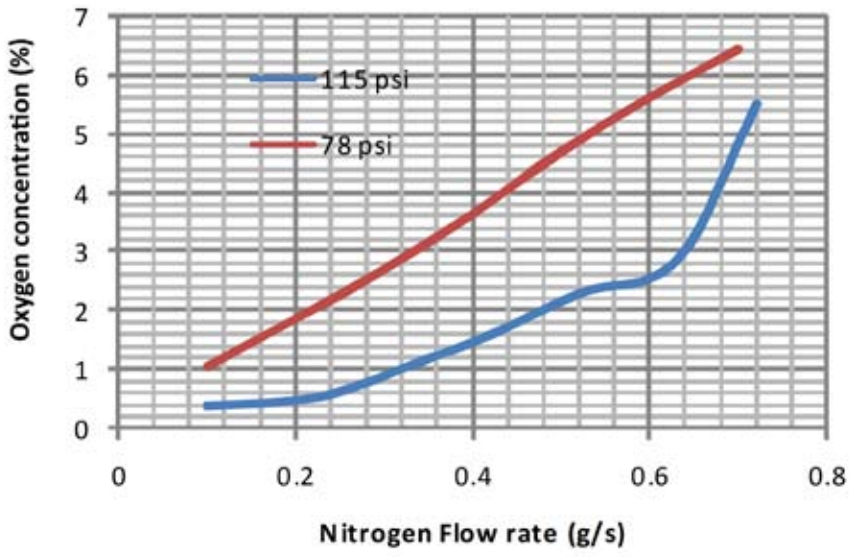

Fig. 2.3.6 Test of Parker membrane for oxygen concentration vs flowrate

2.3.4.3 Practical load map of SRDK-415D GM cryocooler

Two stage GM cryocooler is one of the major components for development of any conduction cooled superconducting magnet system. A 6 T conduction cooled NbTi magnet system has already been developed using a two stage GM cryocooler (Sumitomo SRDK - 415D) of refrigeration capacity of 1.5 W at 4.2 K and 40 W at 50 K. The commercially available typical load map of the SRDK-415D cryocooler shows few 'discrete' points which, in most of the times, is not sufficient to analyze the thermal characteristics of the NbTi magnet system. In this academic year, the practical load map for the SRDK - 415D cryocooler has been generated for both the stages of the GM cryocooler in a test rig. The continuous load curves for both the stages of the cryocooler have been generated. The experimental load map is shown in Fig. 2.3.8.

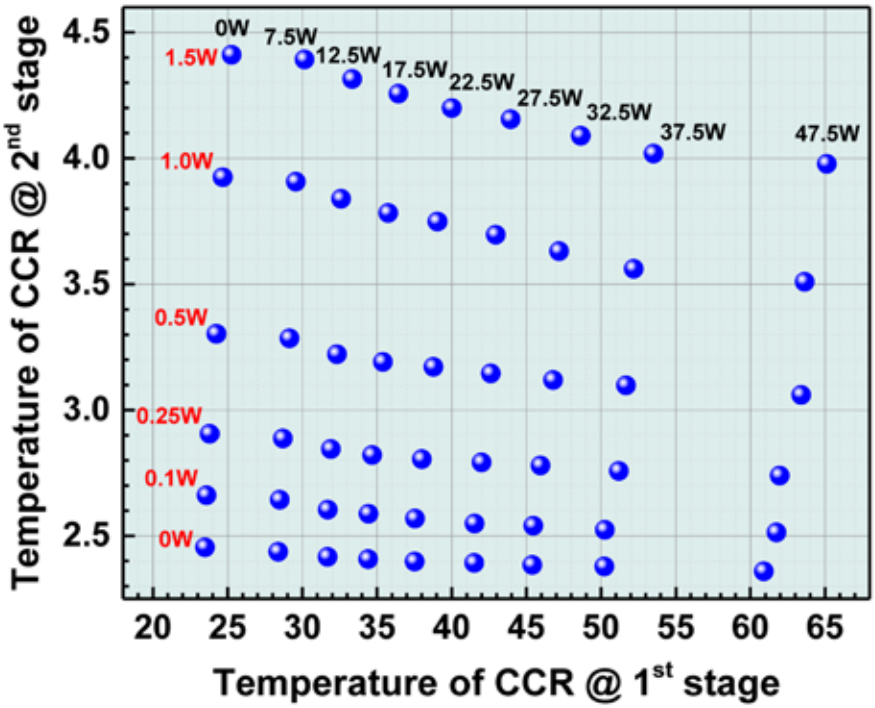

Fig. 2.3.8 Experimental load of two stage GM cryocooler (SRDK-415D)

2.3.4.4 Thermal impedance of electrically insulated thermal joint for hybrid current lead

Hybrid current lead is one of the important parts for the development of cryogen-free or ever-cooled superconducting magnet system.The thermal stability of the cryocooler based NbTi magnet system is greatly dependent on the performance of the hybrid current lead.

Hybrid current lead, which is a combination of the metallic (copper)

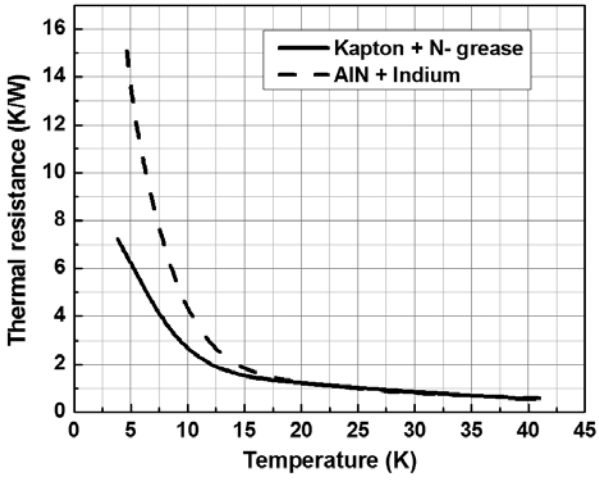

Fig. 2.3.9 Thermal resistance of Cu-AlN-Cu and Cu-Kapton-Cu interface joint in the range of 4-40 K

lead and HTS lead, has some inter-lead joints which need to be electrically insulating and thermally conducting with the different stages of the cryocooler. A thermal anchoring block of oxygen-free high-conductivity (OFHC) copper is developed for inter-lead thermal joint. A detailed experimental study has been carried out using kapton and aluminium nitride (AlN) as interlayer insulation material in the thermal anchoring block. The thermal resistance of the interface for 19 mm2 contact surface area, is found to be ~7 K/W and ~15 K/W for Kapton and Aluminium nitride (AlN) respectively at 4.2 K temperature range and ~0.6 K/W (nearly similar) for both Kapton and Aluminium nitride (AlN) at 40 K temperature range as shown in the Fig. 2.3.9.

2.3.4.5 6 T cryogen-free magnet system (CFMS)

In this academic year, the CFMS has been operated two times for hall measurement. A detail analysis has been done to understand the quench behaviour of the NbTi magnet system using OPERA-3D/ Quench code. The post quench resistance growth has been simulated in the 6 T NbTi magnet along with its current decay and transient temperature rise. Post-quench energy distribution has been extensively studied for the CFMS.

A helium gas circulation based variable temperature insert (VTI) using two stage GM cryocooler (SRDK-408) is under development. Circulating helium gas is cooled by two conduction cooled heat exchangers thermally connected respectively with first and second stages of the cryocooler. A dry scroll pump of 30 m3/h capacity has been used to circulate the helium gas. The minimum temperature at the sample space found to be 15 K which is higher than the desired temperature of 4.2 K. In-line blockage due to the gas contamination is one of the main reasons for not achieving the desired temperature. Necessary modification is going on to achieve desired temperature at the sample space.

2.4 ELECTRONICS FOR CRYOGENICS AND LINAC

Joby Antony and D. S. Mathuria

A. Cryogenic controls: The Crate-less model of control system hardware built out of indigenously built low cost cryogenic instruments (device servers) using ARM processors, interconnected over Ethernet has been operational and is in continuous use for the complete automation of distribution system (CADS) from the cryogenic control room. Two more instruments have been added to the network this year for linac pressure measurements with additional 10 channels. At present twenty six instruments running fifty five embedded servers are operational for control and data acquisition. The cabling between CISCO switches and devices have been modified this year with shielded Molex make cables for better performance.

B. Digital temperature controllers with AC/DC power source and PWM: The expertise gained out of this Ethernet based design has been utilized to make three digital PID devices for temperature controller applications. Digital PID is preferred to analog PID because it is easily programmable for setting any value of P, I, D constants, set points etc. from a PC over LAN. The numbers can be plugged in / programmed on-line with a fractional accuracy like P = 2.121, D = 0.0012. etc. The Fig. 2.4.1 below shows the device and its LabVIEW interface.

Three categories of such devices have been made.

1. **Single channel AC/DC temperature controller using silicon diode as temperature sensor:**

   This is a temperature controller which can be used to maintain constant temperature (between 4.2

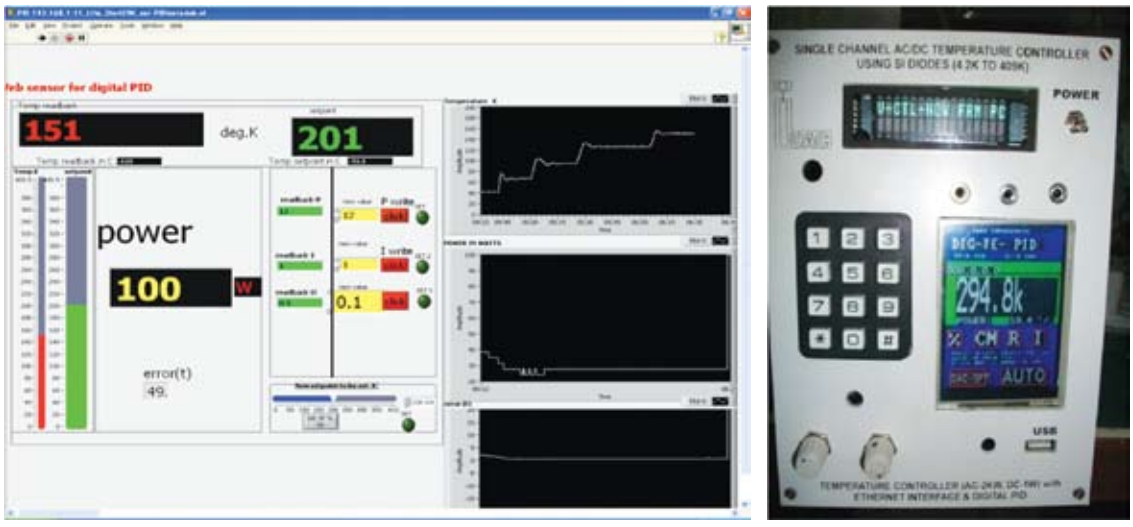

Fig. 2.4.1 The temperature controller device and its LabVIEW interface

K to 409 K) which has also programmable P, I, D bias. This can be used with a variable AC power source (transformer) of upto 2 KW and DC power up to 1 W. This runs a web server with Ethernet interface. LabVIEW interface program is also developed for this. This system has been tested with cryocooler set-up with a precision of ± 0.5 K over twenty four hours.

2. Differential temperature (ΔT) measurement system using silicon diode sensors (4.2 K to 409 K):

This is dual temperature controller unit which has two independent heaters and two silicon diode sensors with independently programmable P, I, D constants etc. The features are same as single channel AC/DC temperature controller. This idea is to use this for ΔT measurements to measure thermal conductivity directly.

3. Single channel digital temperature controller (high temperature):

This is a temperature controller for 0-100 °C applications or higher. In this case, an additional temperature monitor with thermocouple sensor with 0-10 V ouput is required.

C. Software development for low temperature lab

GPIB and RS232 interfacing softwares were developed for instrument interfacing. The following is an interface developed for Oxford make device using LabVIEW.

Fig. 2.4.2 Interface for Oxford make device using LabVIEW

D. The other activities

(i) EBW upgradation

The entire EBW system needed upgrade as most of the parts were obsolete as it was running on Windows 3.11. The machine has been upgraded with new set of PLCs, CNCs, color camera and control electronics. The new control PCs now runs on Windows XP. The team of engineers from M/s Bodycote Techmeta, France was present at IUAC during this work for four weeks.

(ii) SPL laboratory

The newly automated surface preparation facility using Allen bradley PLCs and Intouch Wonderware SCADA needed some minor modifications like software interlocks and user friendly interfaces.

2.5 ECR AND MICROWAVE ION SOURCE DEVELOPMENT LABORATORY

G. O. Rodrigues, Y. Mathur, Narender Kumar, P. S. Lakshmy, R. Becker1, R. W. Hamm2, R. Ahuja, U. K. Rao, R. N. Dutt and D. Kanjilal

[1]Institut fur Angewandte Physik der Universitaet, D-60054 Frankfurt/M, Germany
[2]R&M Technical Enterprises Inc., 4725 Arlene Place, Pleasanton, California 94566, USA

2.5.1 2.45 GHz microwave ion source developments

2.5.1.1 Installation of 2.45 GHz microwave ion source based high flux system for performing experiments related to materials science and plasma physics

A 2.45 GHz microwave ion source based flux system comprising of double-walled water-cooled plasma chamber, permanent magnetic rings for plasma confinement, 4 step ridge waveguide based microwave coupling system for coupling microwave from magnetron head to plasma chamber, 5 electrodes extraction system and an experimental chamber with experimental ladder to mount samples has been installed and commissioned in room no. 127. The source is mounted on a movable rail to make it flexible to handle at the time of maintenance. Fig. 2.5.1 shows the installed system.

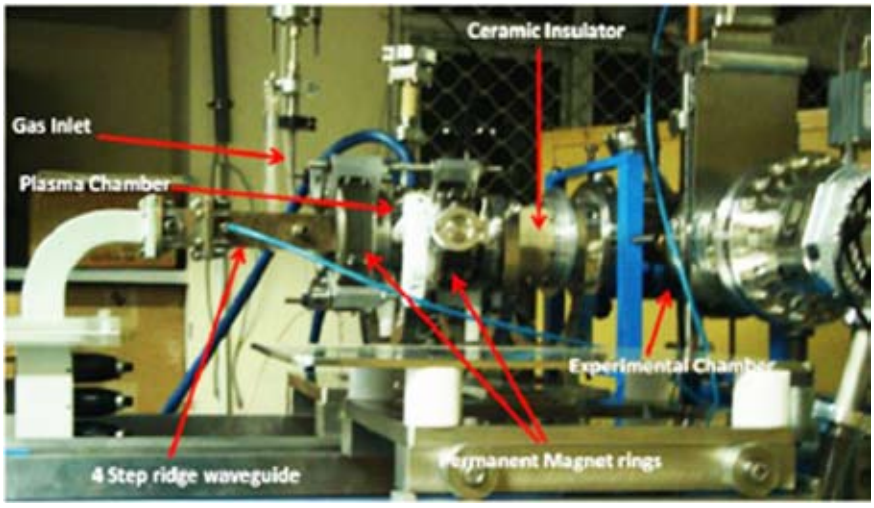

Fig. 2.5.1 View of the 2.45 GHz microwave ion source based high flux system

2.5.1.2 Simulation of the microwave injection line for 2.45 GHz microwave source

Simulation of electric field distribution along the axis of the plasma chamber together with the microwave coupling line using CST Microwave Studio is shown in Fig. 2.5.2 (left and right). Standard WR284 waveguide shown in the left panel of Fig. 2.5.2 was replaced by a 4 step ridge waveguide, as shown in the right panel of Fig. 2.5.2. Simulation (Fig. 2.5.3) shows that the electric field strength at the centre of the plasma chamber is enhanced significantly by a factor of 1.79 in case of the present microwave ion source as compared to the earlier microwave ion source. The use of 4 step ridge waveguide is very useful in terms of maximizing the electric field strength in the centre of plasma chamber as compared to using standard waveguides [1].

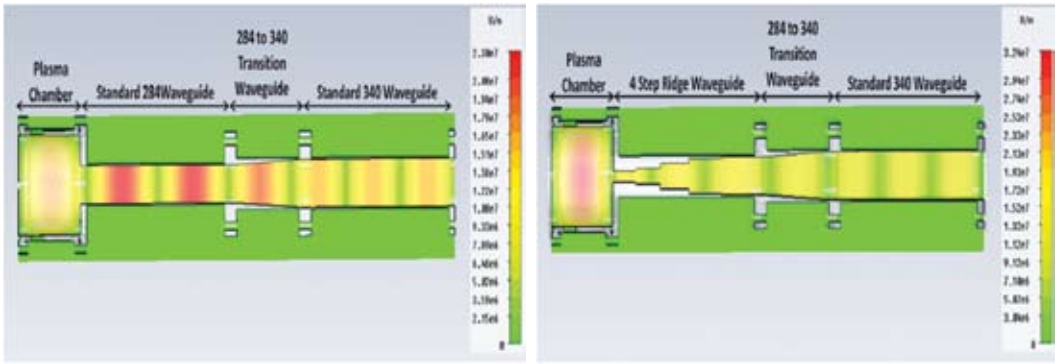

Fig. 2.5.2 (left) Simulated electric field distribution in initial microwave ion source for 1 W input power ; (right) simulated electric field distribution in present microwave ion source for 1 W input power

2.5.1.3 Nitrogen implantation experiment and NRA characterization with analysis

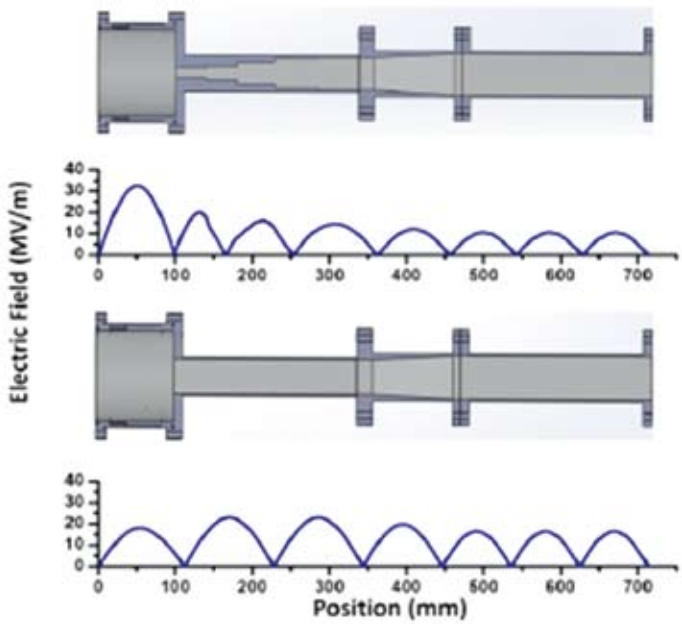

Fig. 2.5.3 Simulated electric field distribution along the axis of the two systems

The nitrogen ion implantation experiment is carried out using the intense ion beam facility developed at IUAC. The silicon samples are mounted on the experimental ladder. The base pressure of the whole system was 1×10^{-6} mbar. The silicon samples are firstly treated with normal angle irradiation of 2 keV Ar^+ ion beam with fluence of 5×10^{16} ions/cm^2 to remove the top silicon dioxide layer. After the completion of top layer removal, the samples are irradiated by N^+ ion beam of energy 10 keV with fluence 1×10^{18} ions/cm^2. The gas pressure during nitrogen ion implantation was kept at 2.3×10^{-5} mbar with 100 W of input microwave power with beam current 23 μA/cm^2.

The extraction voltage is 10 kV with 1.5 mA source current. The samples are then characterized by RBS and NRA, using 2 MeV and 3.694 MeV He^{+2} ion using 1.7 MV Pelletron accelerator at IUAC, to determine the distribution of nitrogen in silicon.

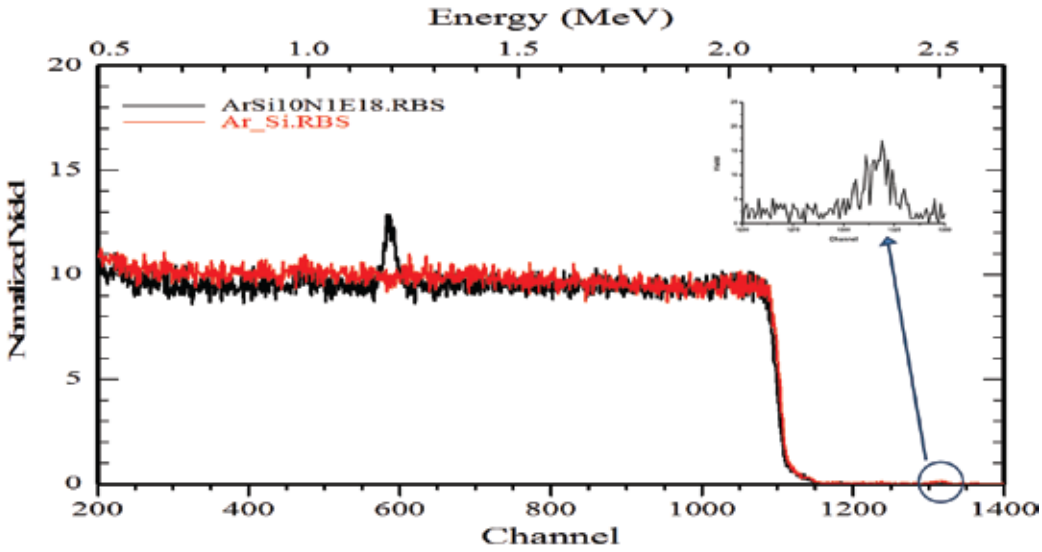

Fig. 2.5.4 NRA spectra for Ar-cleaned (Ar_Si) and for Ar-cleaned-10 keV-N implanted (ArSi10N1E18). The circled portion shows the Ar peak

In Fig. 2.5.4, NRA spectra for Ar ion cleaned silicon (Ar_Si) as well as Ar ion cleaned 10 keV N ion implanted silicon (ArSi10N1E18) with a dose of 1×1018 ions/cm2 are shown. In these two spectra, Ar peak is observed in case of Ar cleaned silicon indicating the implanted Ar ion in silicon matrix, while in the sample cleaned with Ar with same dose and then implanted with nitrogen ions, there is a sharp peak corresponding to nitrogen with no peak for Ar which is due to sputtering due to nitrogen ions. In Fig. 2.5.5, the spectrum is fitted using SIMNRA and RUMP respectively, for nitrogen implanted sample. The simulations shows the nitrogen composition in implanted sample is silicon 20% and nitrogen 80% up to 40 nm which is in accordance to SRIM calculation of 38.4 nm for 10 keV nitrogen implantation in silicon.

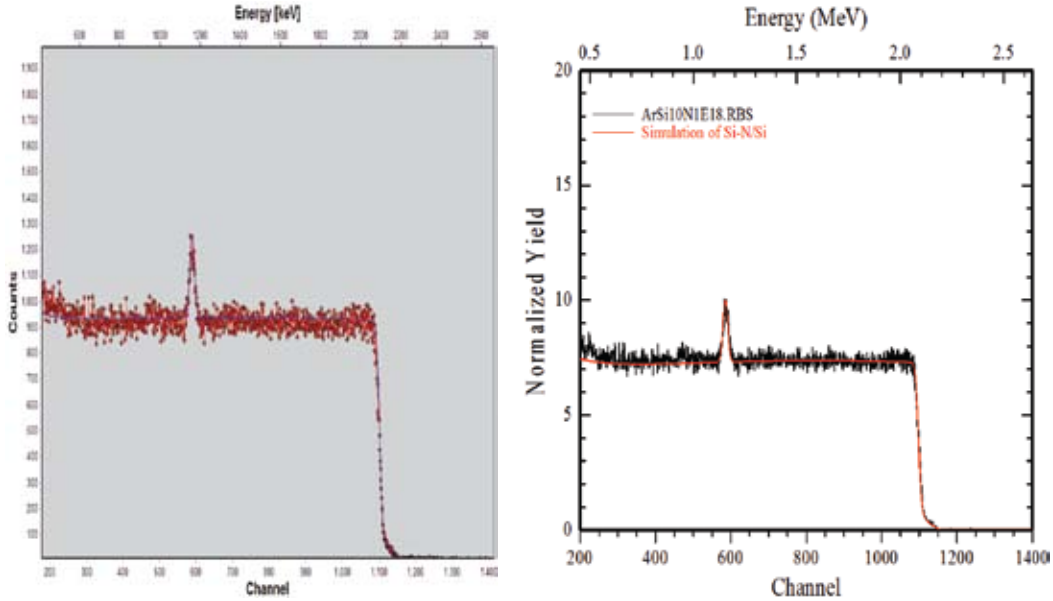

Fig. 2.5.5 (left) NRA spectrum of 1E18 N+ ion implanted Ar+ ion cleaned silicon (red line) and fitted spectrum using SMINRA (blue line); (right) NRA spectrum of 1E18 N+ ion implanted Ar+ ion cleaned silicon (red line) and fitted spectrum using RUMP (Blue line)

2.5.2 Study of the frequency tuning effect with simulations using CST particle tracking solver

The frequency tuning effect in ECR ion sources has become a useful technique to improve the performance of existing ion sources and was pioneered by the ECR group at Catania, Italy. Generally, the electromagnetic field distribution inside a cavity depends on the frequency and is preserved even in the presence of the plasma. Additionally, the ECR surface can get modified in terms of its dimension and shape which can further influence the beam intensity, shape, emittance, and brightness. Due to the remarkable changes in the beam characteristics, the quality of the beam can be improved further. In order to further understand the evolution of the measured beam shapes as a function of frequency, particle tracking under the combined influence of the confining magnetic field and rf electric field was initiated [2]. For this purpose, the CST particle studio program was used. It incorporates a powerful electromagnetic solver for calculating external fields, it has an efficient particle tracking algorithm and sophisticated emission models that can describe the extraction of particles from active surfaces.

The magnetic structure with the cavity was used for particle tracking inside the cavity without considering the effect of the plasma (Fig. 2.5.6). The dominant mode of the ECR cavity was chosen for tracking the motion of electrons and to further compare it with the measured distribution of the beam shape at the particular frequency of 10.11 GHz. The left panel of Fig. 2.5.7 shows the evolution of the electrons from the DC bias tube at a voltage of 100 V as viewed from the injection side and showing the quadrupole shape of the plasma. The electrons can quickly gain energy of ~ 600 keV in ~ 7.7 ns. The simulated shape of the ECR plasma matches reasonably well with the measured shape of the beam for the dominant mode, as shown in the right panel of Fig. 2.5.7. The particle tracking in the vacuum mode cavity shows the evolution of the quadrupolar structure of the ECR plasma which is similar to the measurement of the beam shape at the dominant mode. This shows that the electromagnetic field distribution affects the shape of the ECR plasma at a particular mode of operation.

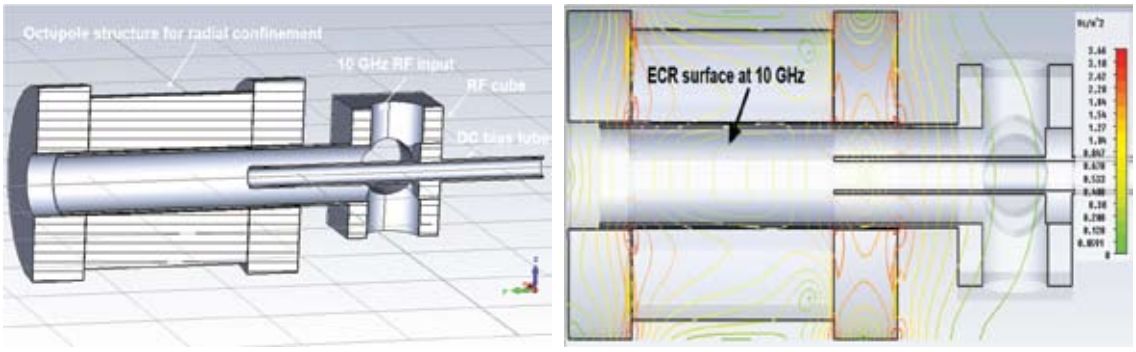

Fig. 2.5.7 (left) View of the computed electron trajectories at the injection side with initial energy of 100 eV for the dominant mode in vacuum; (right) measured shape and intensities of the beam for oxygen plasma for various frequencies before mass analysis (top) and after analysis (bottom) for O5+ (BPM sensitivity ; before analysis 10-4 A/V ; after analysis 10-6 A/V)

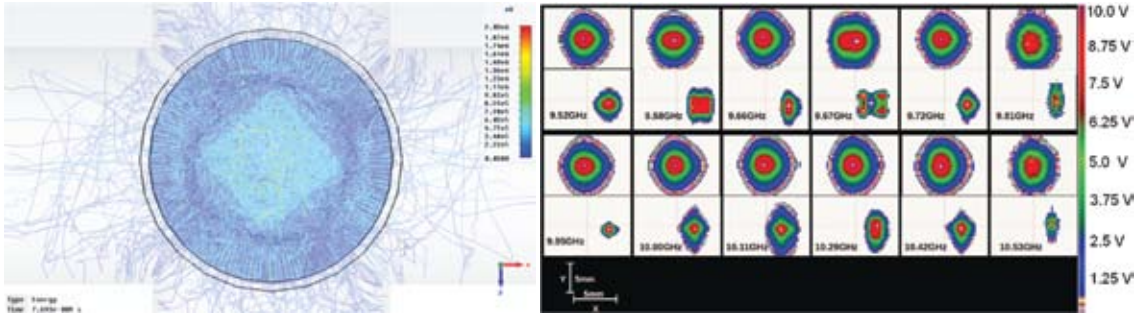

Fig. 2.5.7 (left) View of the computed electron trajectories at the injection side with initial energy of 100 eV for the dominant mode in vacuum; (right) measured shape and intensities of the beam for oxygen plasma for various frequencies before mass analysis (top) and after analysis (bottom) for O^{5+} (BPM sensitivity ; before analysis 10^{-4} A/V ; after analysis 10^{-6} A/V)

2.5.3. Direct injection of intense, heavy ion beams from a high field ECR ion source into an RFQ

Beam intensities achievable from high performance ECR sources for highly charged ions are limited by the high space charge. For high performance ECR sources, the stray magnetic field of the source can provide focusing against the space charge blow-up of the beam when used with the Direct Plasma Injection Scheme (DPIS) developed for laser ion sources. A combined extraction/matching system has been designed for direct injection into a radio frequency quadrupole (RFQ) accelerator, allowing a total beam current of 12 mA for the production of highly charged 238U40+ (0.49 mA) to be injected at an ion source voltage of 60 kV (Fig. 2.5.8). In this design, the features of IGUN have been used to take into account the rf-focusing of an RFQ channel (without modulation), the electrostatic field between ion source extraction and the RFQ vanes, the magnetic stray field of the ECR superconducting solenoid, and the defocusing space charge of the ion beam. The RFQ has been designed [3] to suppress most of the charge states extracted from the ECR, acting as a filter for the desired 238U40+. This reduces the transport problem for the beam line as well as reduces the emittance for the transmitted charge states.

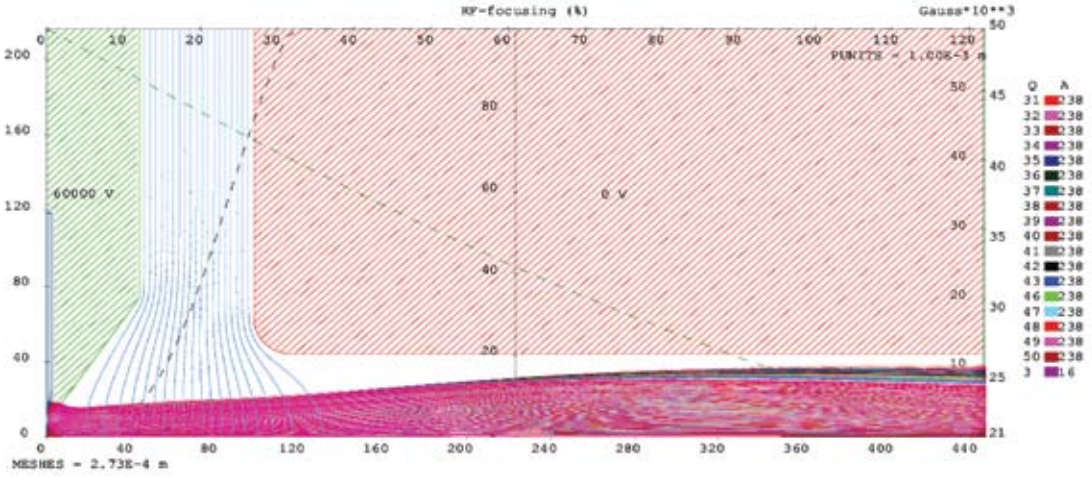

Fig. 2.5.8 Optimized design for transporting a total current of 12 mA (from a 56 GHz ECR source), consisting of U^{40+}, other U^{+} charge states, and oxygen mixing gas ions directly into an RFQ

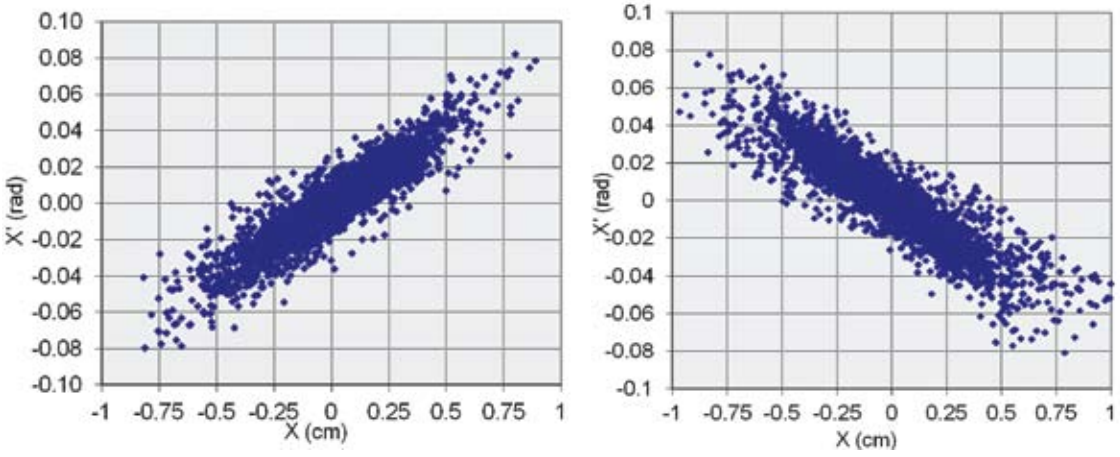

Fig. 2.5.9 (left) the calculated output phase space in the x plane of the U^{+40} charge state extracted from the 56 GHz ECR and transmitted through the RFQ; (right) the same in the y plane

It is evident that such an RFQ-channel might be very effective and less q/m sensitive for the extraction system of all high performing ECR ion sources. This technique has promising applications for injecting and transporting very intense beams into RFQ accelerators for research, ADSS and more efficient, compact neutron generators. The accelerator driven sub-critical system (ADSS) being developed at various laboratories around the world to create nuclear energy may also benefit from this technique, both in terms of transporting intense beams of protons and making the low energy segment more compact. This RFQ is essentially a buncher configured as a charge filter, so RIB facilities can take advantage of this technique. The charge breeding concept can be utilised with a powerful ECR ion source directly coupled to this RFQ charge filter and then injected into an another higher frequency RFQ for additional acceleration.

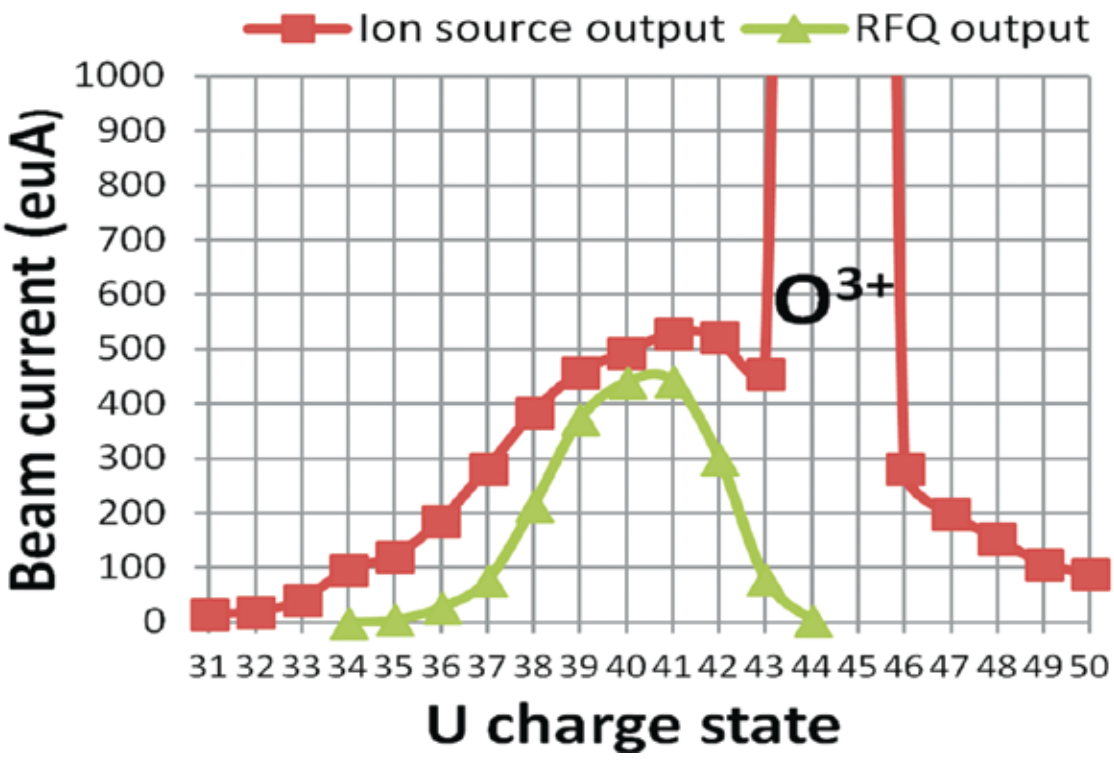

Fig. 2.5.10 The scaled U^{+} charge states extracted from the 56 GHz ECR and the calculated charge states transmitted through the RFQ.

REFERENCES

[1] N. Kumar, G. Rodrigues, Y. Mathur, P. S. Lakshmy, R. Ahuja, R. N. Dutt and D. Kanjilal, IPAC 2014, Dresden, Germany, MOPRI008

[2] Frequency tuning effect on the bremsstrahlung spectra, beam intensity, and shape in an ECR ion source, Proceedings of the 21st International Workshop on ECR Ion Sources, ECRIS 2014, Nizhny Novgorod, Russia, August 2014; http://accelconf.web.cern.ch/AccelConf/ECRIS2014/html/sessi0n.htm

[3] Direct injection of intense heavy ion beams from a high field ECR ion source into an RFQ, Proceedings of the 21st International Workshop on ECR Ion Sources, ECRIS 2014, Nizhny Novgorod, Russia, August 2014; http://accelconf.web.cern.ch/AccelConf/ECRIS2014/html/sessi0n.htm